AN ABSTRACT OF THE THESIS OF

_____Brooke Molson-Moran_____ for the _____Master of Science_____ Degree

in _____Physical Sciences_____ presented on _____

Title: Investigating Seasonal Impacts on Subsurface Salinization in Northeastern Thailand

with Electrical Resistivity Tomography_____

Thesis Chair: Dr. Marcia Schulmeister

Abstract approved: _____
(Thesis Advisor Signature)

Salinization of groundwater resources can be characterized using Electrical Resistivity Tomography (ERT) but has not been fully evaluated in aquifers that are impacted by cyclic and long-term trends in monsoon rainfall. Groundwater and soil salinization in northeastern Thailand is associated with dissolution of rock salt layers in the Mahasarakham Formation, a Cretaceous sedimentary sequence usually containing three layers of rock salt. While parts of the overlying unconsolidated aquifer produce high-quality fresh water, others produce brackish to saline water. We evaluated two ERT profiles obtained from fresh and saline aquifers near Khon Kaen, Thailand to consider the importance of seasonal water levels and ground water salinity in ERT interpretations. Seasonal differences in water depths and specific conductance were monitored in existing irrigation and domestic supply wells where associated lithologic logs were available. Between the rainy and dry seasons, average groundwater depths differed by 5 meters and 10 meters at fresh and saline sites, respectively. From the rainy to the dry season, differences of 34 µS/cm and 97 µS/cm were observed in specific conductance at fresh and saline sites, respectively. The ERT profiles are characterized by horizontal layers with higher resistivity in the uppermost layer and lower resistivity in the underlying layer. Water-level depths at both sites do not coincide with the positions of steep ERT resistivity gradients observed at 2.5 m and 5 m at the fresh and saline sites. Fine-grained soil textures at both locations are likely to promote capillary rise and the upward migration of saline pore water in unsaturated sediments, which can significantly influence ERT resistivity patterns. Modelled capillary rise estimates are consistent with the positions of steep ERT resistivity gradients at both locations. The results indicate that seasonal and long-term water-level trends should be considered when evaluating resistivity measurements in saline subsurface conditions, which are essential to successful salinity management.

INVESTIGATING SEASONAL IMPACTS ON SUBSURFACE SALINIZATION IN

NORTHEASTERN THAILAND WITH ELECTRICAL CONDUCTIVITY

TOMOGRAPHY

A Thesis

Presented to

The Department of Physical Sciences

EMPORIA STATE UNIVERSITY

In Partial Fulfillment

of the Requirements for the Degree

Master of Science

----

by

Brooke Ann Molson-Moran

November 2021

Thesis approved by:

_____
Dr. Marcia Schulmeister, Committee Chair

_____
Committee Member

_____
Committee Member

_____
Department Chair

_____
Dean of the Graduate School and Distance
Education

ACKNOWLEDGEMENTS

TABLE OF CONTENTS

LIST OF TABLES

LIST OF FIGURES

CHAPTER 1

INTRODUCTION

Measurement of the electrical properties of water, soil, and rock is commonly conducted when evaluating soil and groundwater salinity. The electrical conductivity of water and resistivity of geologic media are both measures of how well a material conducts electricity. Given that both techniques measure the same physical property, their uses in a common medium should provide complementary information about subsurface conditions. The conductivity of water samples can be measured directly and provides information on fluid salinity. Electrical resistivity tomography (ERT) is a geophysical technique used to assess the resistivity of subsurface soil and aquifer materials. Since resistivity in geological materials is dependent on clay content, saturation state, and salinity, hydrochemical measurements of fluids, along with an accurate understanding of relevant geology, are essential for interpretations made using electrical resistivity tomography interpretation.

Over 10,000,000 km^2 of the Earth's soil surface is affected by high salinity (Food and Agriculture Organization of the United Nations and Intergovernmental Technical Panel on Soils, 2015). Highly saline soil and groundwater pose threats to drinking and irrigation water supplies, agriculture, and infrastructure in more than 100 countries, including the United States and Thailand (Food and Agriculture Organization of the United Nations and Intergovernmental Technical Panel on Soils, 2015). High salt concentrations in soil and water are often caused by natural dissolution of mineral sources and geochemical processes. However, human activities such as deforestation, groundwater

overuse, soil disturbance, and dam-building contribute to salt-affected soil (Arjwech et al., 2018; Löffler and Kubiniok, 1988; Hall et al., 2004). In Thailand, 19,000 km^2 of inland saline soils exist (Arunin and Pongwichian, 2015). In Khon Kaen Province, 3,360 km^2 of soil is affected by salinity (Arjwech et al., 2020). In the Khon Kaen drainage basin, the amount of total dissolved solids in the groundwater is between 100 and 44,000 mg/L, a range considered to be very fresh to levels higher than in average seawater (Srisuk, 1996; U.S.G.S., 2021).

The city of Khon Kaen in northeastern Thailand has recently undergone significant urban salinization. In the topographic uplands west and north of Khon Kaen, groundwater dissolves deep bedrock halite deposits (Löffler and Kubiniok, 1988). As urban areas are developed, tree removal in upland areas has resulted in salinization of soils in the lowlands at lower elevations in the southeast of the study area (Löffler and Kubiniok, 1988). The removal of vegetation eliminates the water loss by water uptake by roots and by evapotranspiration, resulting in a rise in the water table elevation (Löffler and Kubiniok, 1988). The result is an increase in saline groundwater as it is introduced into the overlying unsaturated zone via capillary rise, as saline groundwater levels are elevated (Löffler and Kubiniok, 1988). The urban salinity problem in Khon Kaen threatens the development of new infrastructure and preservation of historic buildings, in addition to limiting agricultural practices.

A combination of hydrological and geophysical research is necessary to understand the mechanisms responsible for the salinization of salt-affected regions (Haworth et al.,

1959; Srisuk, 1996). Previous studies using electrical resistivity tomography (ERT) have been conducted in Khon Kaen, Thailand that examined the origin and extent of salt-affected soils and groundwater in and around Khon Kaen (Arjwech et al., 2018; Arjwech et al., 2019; Arjwech et al., 2020). The previous work forms the foundation of this study.

1.1 Research Objectives and Hypotheses

This work will test the hypothesis that ERT can be used to identify the top of the water table in fresh-water aquifers, and that, where saline groundwater exists, ERT will predict the top of the capillary zone. To evaluate these questions, ERT profiles, groundwater chemistry, and water table measurements were compared at two locations where fresh and saline groundwater have been observed. Given their significant influence on resistivity, small-scale variations in sediment lithology at both locations were evaluated. ERT surveys were conducted to assess subsurface soil, rock, and groundwater resistivities. Groundwater samples and water table depths were obtained in wells adjacent to the ERT profiles and were used to identify the top of the water table and groundwater salinity. Sediment textures were indicated in lithologic logs obtained from the Thailand Department of Groundwater Resources (2019) water well database and were used in predictions of capillary rise that may occur at each location. The region experiences monsoon climatic rainfall conditions, which may affect the water table level and ground water chemistry. To evaluate the possible seasonal variations in these parameters, groundwater samples and water-level measurements were obtained during both dry and rainy seasons from a set of select representative wells within the study area.

CHAPTER 2

BACKGROUND

2.1 Geographic Setting

The city of Khon Kaen in northeastern Thailand spans approximately 46 km^2 in Khon Kaen Province (Figure 2.1). As of 2017, the population of Khon Kaen Province was more than 1.8 million, and in 2015, the city of Khon Kaen had a population of 118,262 (Office of the National Economic and Social Development Council, 2017). Over the past several decades, land use has shifted from primarily agriculture to urban development and sprawling suburban communities, due to population growth (Arjwech et al., 2019).
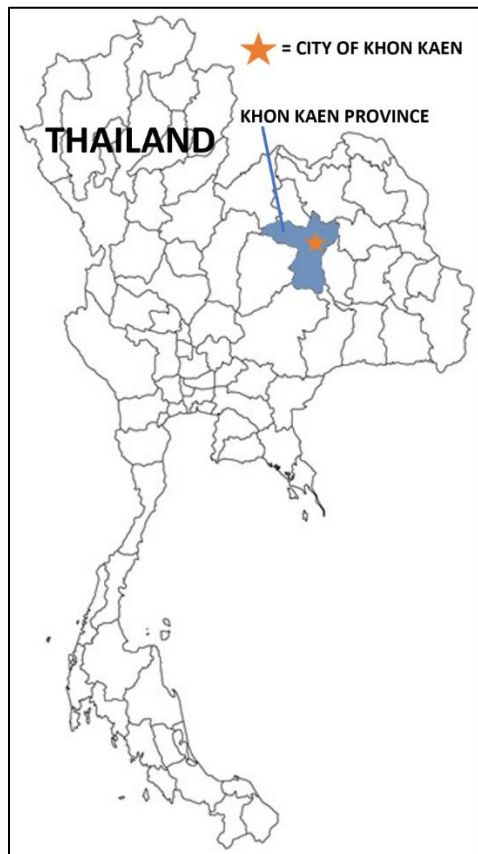
Figure 2.1 Khon Kaen Province and the city of Khon Kaen, in northeastern Thailand.

2.2 Regional Geology

The city of Khon Kaen lies within the Khorat Plateau, a structural geologic feature in northeast Thailand (Figure 2.2). The Khorat Plateau can be subdivided into two basins: the Sakhon Nakhon Basin to the north and the larger Khorat Basin in the south, separated by the Phu Phan Mountain Range. The city of Khon Kaen lies within the Khon Kaen subbasin, which is located on the western edge of the Khorat basin (Arjwech et al., 2019). This basin exhibits south and southeast plunging north-northwest and south-southeast trending syncline and anticline axes (Srisuk, 1996). Faulting in the basin is oriented northeast and north to northwest, and many rivers, such as the Chi and Phong Rivers, are positioned along these fault lines (Srisuk, 1996).
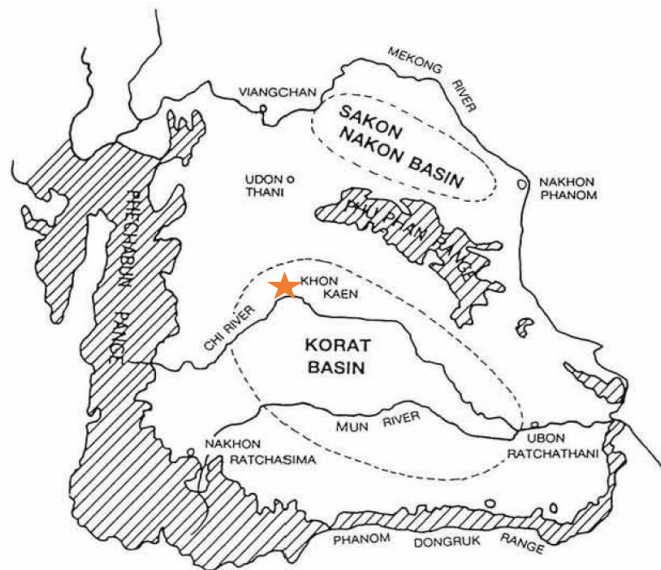
Figure 2.2 The Khorat Plateau with the city of Khon Kaen near the center. The city (orange star) is situated north of the Chi River and within the Khorat Basin (Wada, 2005).

Geologic structures and man-made impoundments are known to influence the

distribution of soil and groundwater salinity in the region. Geologically, formation contacts and contacts of folded strata can control the movement of groundwater (Arjwech et al., 2018). High salinity has been reported west of the city of Khon Kaen at the contact between the Mahasarakham Formation and the underlying Khok Kruat Formation (Raksaskulwong and Monjai, 2007). These layers dip gently to the east, and groundwater flows in an eastern and southeastern direction. Rock salt layers at the top of the Mahasarakham Formation are dissolved by groundwater and ions move upward to the ground surface and along the direction of groundwater flow (Arjwech et al., 2019). The presence of anticlines corresponds with severe salinity at the surface (Arjwech et al., 2019). The rock salt forms domes, as an analogous structure in relation to anticlines and likewise, forms depressions above synclines (Arjwech et al., 2019).

Bedrock in the study area consists of a sedimentary series, the Khorat Group, which dips between five and twenty degrees to the east (Srisuk, 1996). The older formations of the Khorat Group are roughly 1200 meters of interbedded shale and sandstones, with a range from fine-grained to boulder-sized conglomerates (Lamoreaux et al., 1958). The Mahasarakham Formation, the uppermost formation of the Khorat Group, consists of clay, shale, sandstone, and from one to three layers of evaporites, including halite (Figure 2.3). The undulating Mahasarakham Formation layers are 250 m thick on average but varies from 10 m up to 1 km meters (Arjwech et al., 2018; Shen et al., 2021). The evaporites within the Mahasarakham Formation are more than 1000 m thick in some areas (Shen et al., 2021). The evaporite layers form large doming structures in some places and pinch out in others (Figure 2.4). These evaporites, particularly the halite, or rock salt, are the source

of the region's salinity and the thickness and their depth has is a major influence on the local soil salinity (Arjwech et al., 2018).

The Mahasarakham Formation is overlain by the Tertiary Phu Tok Formation. The Phu Tok Formation is mainly composed of sand, gravel, purple sandstone, and shale, and is overlain by Quaternary deposits. Proponents of newer nomenclature consider the Phu Tok Formation to be the upper layer of the Cretaceous Mahasarakham Formation.

ERA	TIME SCALE	SYSTEM PERIOD	SERIES EPOCHS	LITHOLOGY	FORMATION	GROUP	DEPOSITIONAL ENVIRONMENTS	TECTONIC EPISODES
CENOZOIC		Quaternary		Gravel	Unnamed		Alluvial	
	2.0	Tertiary		Siltstone Mudstone	Phu Tok		Fluviatile	India collides with Asia-Folding of Khorat Plateau
MESOZOIC		Cretaceous		Rock salt Mudstone	Maha Sarakham		Evaporitic	
				Sandstone Shale	Khok Kruat	K H O R A T	Fluviatile	
				Sandstone	Phu Phan		Fluviatile	
	144	Jurassic	Upper	Sandstone	Sao Khua		Fluviatile	Interior Sag
			Middle	Sandstone	Phra Wihan		Fluviatile	
			Lower	Sandstone	Phu Khradung	G R O U P	Fluviatile	
	190	Triassic	Upper Rhaetian	Shale Sandstone	Nam Phong		Fluviatile	
			Upper Norian-Carnian	Shale Sandstone	Lower Nam Phong (Huai Hin Lat)		Fluviatile	Khorat Unconformity
	200		Middle Lower-	L.S Conglomerate	Triassic Fill		Fluvio-Lacustrine	Indosinian Orogeny

Clastics U Unit (<680 m) — Upper Member
Halite U Unit (2 m)
Anhydrite Marker Unit 3 (0.5 m)
Halite U Unit (20-70 m)
Clastics M Unit (20-70 m) — Middle Member
Halite M2 Unit (10-70 m)
Anhydrite Marker Unit 2
Halite M1 Unit (20-60 m)
Clastics L Unit (10-60 m) — Lower Member
Potash Unit (10-75 m)
Halite L2 Unit (10-200 m)
Anhydrite Marker Unit 1(0.5-3 m)
Halite L1 Unit (30-350 m)
Basal Anhydrite Unit (1.1 m)
Top of Khok Kruat Formation

Figure 2.3 Left: General stratigraphy and lithology underlying Khon Kaen, Thailand. Right: Lithostratigraphy of the Mahasarakham Formation. (El Tabakh et al., 1999).
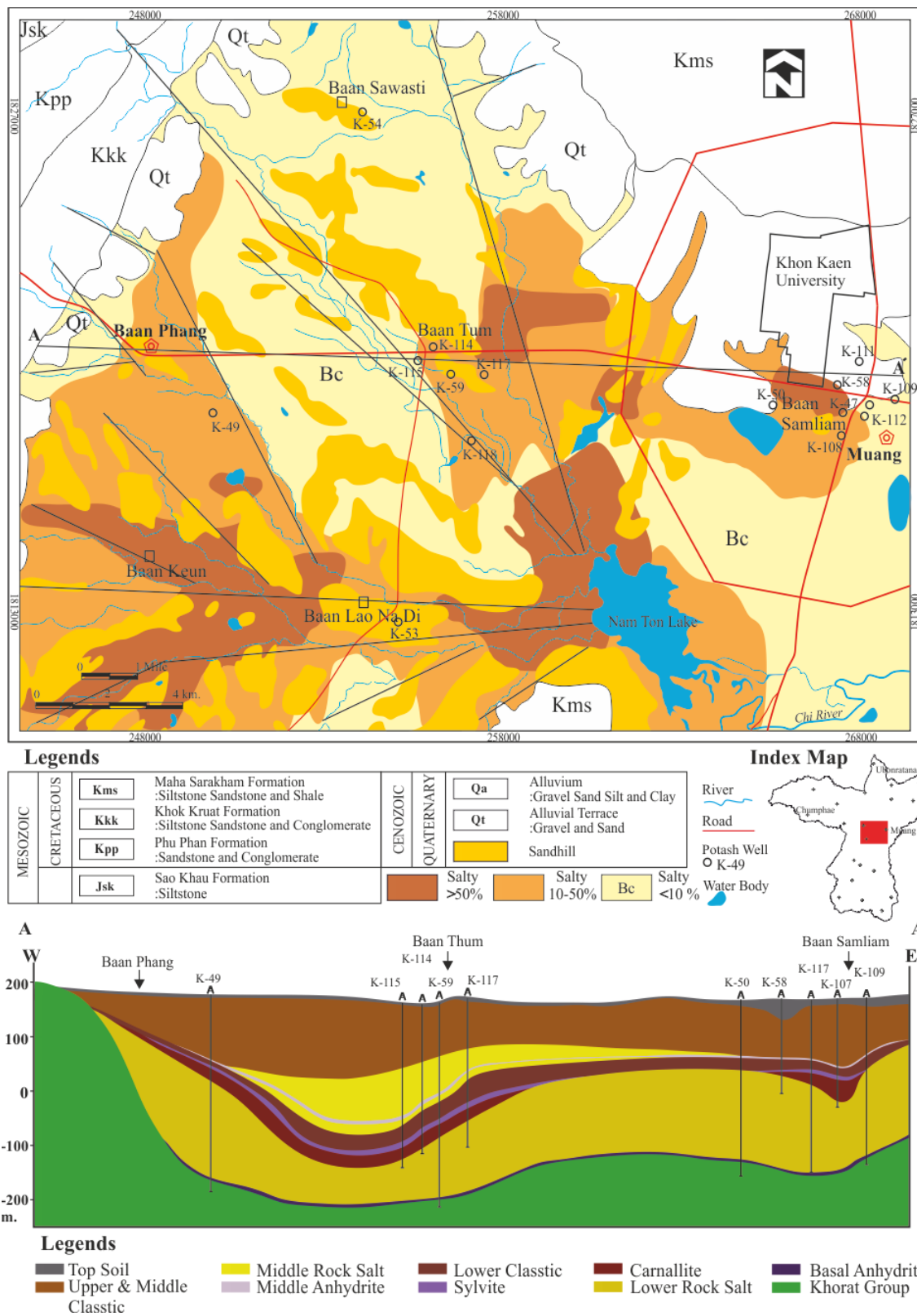
Figure 2.4 Location map and generalized geologic cross section of west of Khon Kaen to the city center (Arjwech et al., 2020).

The Quaternary deposits are stratigraphically complex due to a history of river and floodplain migration, sediment deposition, and erosion. The unconsolidated deposits are laterally variable with interbedded alluvial clay, sand, and gravel, and with minor laterite beds and lateritic soils. Distinct clay layers vary by their differences in color and texture (Thailand Department of Groundwater Resources, 2019). The thickness of the Quaternary deposits ranges from 0 to 80 meters thick (Lamoreaux et al., 1958; Raksaskulwong and Monjai, 2007). Finer-grained sand and clay, deposited by water that carved into the existing sand and gravel deposits, make up most of the basin's center.

Some geologists classify the Quaternary deposits into low, middle, and high terraces, but other interpretations rule out the three-layer terrace model due to the presence of horizontal deposits that were likely not deposited by water (Boosener, 1985; Löffler and Kubiniok, 1988; Raksaskulwong and Monjai, 2007). Others propose that, despite areas of fluvial deposition, some landscapes are a result of erosional processes and represent weathered land surfaces (Löffler and Kubiniok, 1988). Regardless of disagreement concerning classification and provenance, there are at least two distinct varieties of Quaternary deposits, and both are observed in quarry outcrops. The Quaternary sediments are often divided into terrace (Qt) and alluvial (Qa) deposits.

Qt deposits are primarily composed of gravel and sand, represent floodplain deposits from the ancestral Phong and Chi Rivers, and are found at the margins of the Khon Kaen basin (Raksaskulwong and Monjai, 2007) The Qt deposits are located in the eastern part of the study area, are at higher elevations and are older than the alluvial, Qa deposits.

Qt deposits include cobbles, pebbles, sand, some clay, loess, and laterite, along with locally abundant petrified wood and rare tektites (Raksaskulwong and Monjai, 2007). However, some stratigraphic descriptions do not document the loess or laterite. The upper Qt layers are mainly red with some pink to orange soil and contain pisolites near the surface (Boosener, 1985). Other layers include pale gray, yellow to buff and red to pinkish-orange silty sand with ferricrete lenses. Tektites and petrified wood in terrace deposits have been dated at between 700,000 and 900,000 years B.P. (Raksaskulwong and Monjai, 2007). The alluvial Qa material was deposited by stream channels that incised linearly through the Qt sand and gravel deposits. These sediments make up most of the basin's center. Qa sediments are generally finer grained than Qt deposits and include clay, silt, sand, and some gravel (Raksaskulwong and Monjai, 2007).

Depending on the author, the term "laterite" may represent a variety of earth materials: from simply an iron-rich soil, to clays which dry out when exposed to air, to rocks with specific compositions and origins. Geologically, laterite is a sedimentary rock formed by secondary processes in humid, tropical environments with distinct wet and dry seasons (Yamaguchi, 2020). It usually develops as a product of the weathering of stratigraphically lower parent material, which can be virtually any type of iron-rich rock (Yamaguchi, 2020). Laterite forms in a reaction zone, where rock and water interact and extends from the minimum to the maximum water table levels (Yamaguchi, 2020). During the wet seasons, rock is leached of ions, specifically Na, K, Ca, and Mg ions (Yamaguchi, 2020). The solution containing these ions often dissolves SiO_2 instead of iron oxides, resulting in an iron-rich laterite (Yamaguchi, 2020).

Boonsener (1985) classifies the laterite in and around Khon Kaen into three categories: gravelly, pisolithic, and massively bedded. The gravelly laterite occurs outside of the study area, east of Khon Kaen, and the pisolithic and massively bedded laterite occurs within the study area (Boonsener, 1985). The pisolithic laterite is approximately a one-meter layer of pea-sized brownish-black iron oxide concretions mixed with silt and clay (Boonsener, 1985). The massively bedded laterite layer is also about one-meter thick, well-cemented iron oxide, and reddish brown to brownish black in color (Boonsener, 1985).

Loess is a silty to sandy, often carbonaceous, sediment usually formed by aeolian deposition. It occurs in some areas of upper terrace deposits and can be over 5 meters thick (Raksaskulwong and Monjai, 2007; Arjwech et al., 2019). Charcoal found in loess deposits within 100 km of Khon Kaen have yielded dates of 8,190 and 6,620 B.P. (Raksaskulwong and Monjai, 2007).

2.3 Surface Water

The city of Khon Kaen is located in the Chi River sub-basin, the third largest catchment area in the country, with an area of 49,476 km2 (Food and Agriculture Organization of the United Nations, 2016). The city is located west of the confluence of the Phong and Chi Rivers and north of the Mun River (Figure 2.5). The Chi River, the longest river entirely within Thailand, flows east through Khon Kaen eventually flowing into the Mun River, a tributary of the Mekong River. Ubolratana Reservoir, with a storage

capacity of 2,431 million cubic meters, lies northwest of the city (Electricity Generating

Authority of Thailand, 2013). Nok Iang Reservoir is southwest of the city center.

Srisuk (1996) found that precipitation dilutes salinity in rivers during the rainy

season. Specifically, the Chi River had a TDS content of 132 mg/L during the rainy season

as opposed to 714 mg/L during the summer (Srisuk, 1996). River water from the Chi and

Phong Rivers is more saline during the rest of the year due to groundwater discharge into

the rivers, as groundwater on either side of the rivers was considerably more saline than

the rivers themselves (Srisuk, 1996).
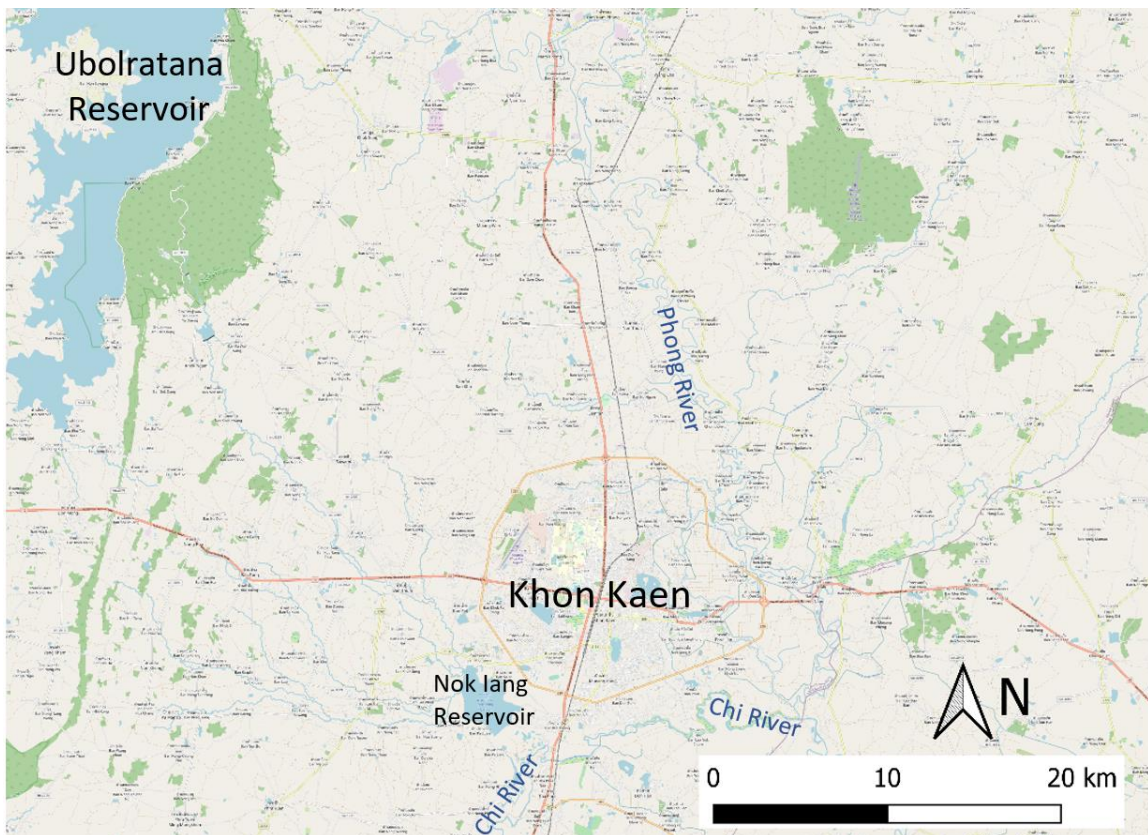
Figure 2.5 Khon Kaen, Thailand and surrounding area. The city is at the intersection of

two major roads. Geographical features include a large reservoir to the northwest of the

city, several large rivers, many smaller streams, and swampy areas, particularly to the south, but also in the city center. Map made using QGIS software (QGIS, 2019).

2.4 Groundwater Hydrology

2.4.1 Aquifer Resources

Quaternary layers in and around Khon Kaen support important freshwater aquifers, given their poorly sorted alluvial nature (Wongsawat et al., 1992). However, in some areas the water may be too saline for consumption. The wells located in the western part of the study area are completed in Quaternary alluvial (Qa) deposits and are listed by the Department of Ground water Resources as S1710, S1735, F471, Y948, and KK101 (DGR, date; Figure 2.6). The wells in the eastern portion of the study area are completed in Quaternary terrace (Qt) deposits and include wells F1599, DP421, F1600, F1593, KK91, DP465, RTB174, TX210, F186, Y1905, S1863, F823 (Figure 2.6). Groundwater of the Khorat Plateau flows in an eastern direction and near Khon Kaen, in a southeastern direction (Wongsawat et al., 1992).
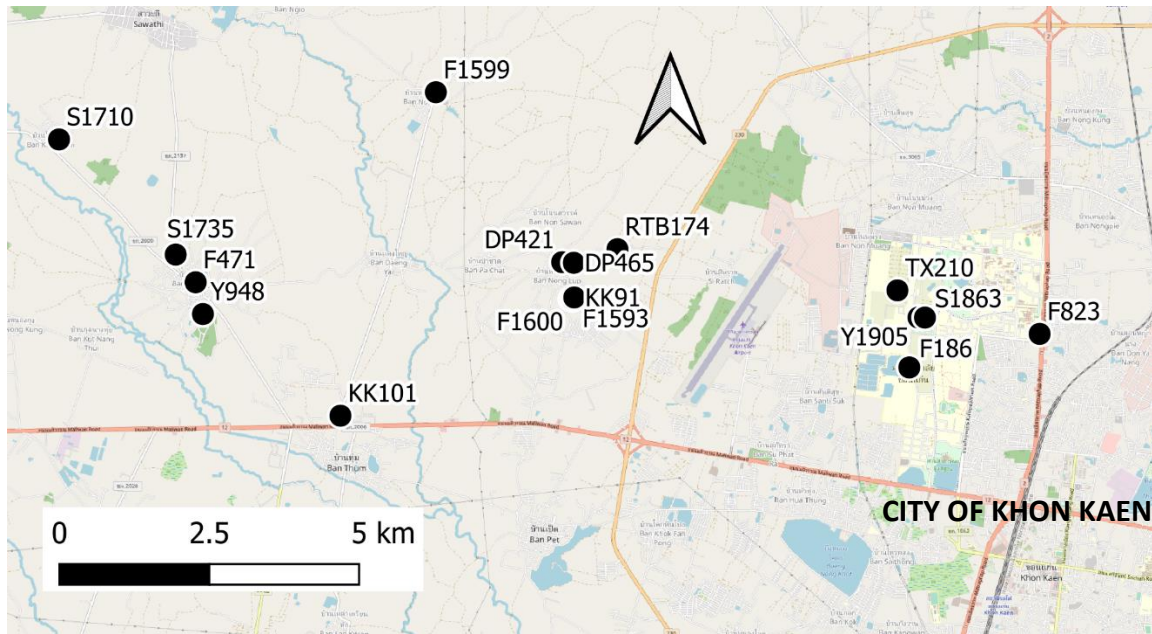
Figure 2.6 Map of the study area in Khon Kaen, Thailand labelled with the names of Thailand Department of Groundwater Resources wells. The wells in the western part of the study area are in Quaternary alluvial deposit and depicted with light yellow and yellow without a border, or the Phu Tok Formation. Wells in the eastern part of the study area are in Quaternary terrace deposits (yellow and are outlined) or the Phu Tok Formation (QGIS, 2019; Arjwech et al., 2018).

Five of the eight consolidated sedimentary formations of the Khorat Group are considered useful as aquifers (Srisuk, 1996). Some units in the upper Khorat Group have low porosity and low productivity (Williamson et al., 1989). The Mahasarakham Formation contains soluble rock salt layers that dissolve to produce saline groundwater. The saline groundwater migrates into adjacent formations, especially the Quaternary deposits (Wongsawat et al., 1992). The evaporite layers of the Mahasarakham Formation are the primary source of salinity of the region's saline soil and groundwater (Löffler and

Kubiniok, 1988).

The Quaternary deposits and Phu Tok Formation may be characterized as confined or unconfined aquifers depending on local lithology, specifically the presence of confining clay layers, and distance from stream recharge areas (Buaphan et al., 1995). Deep aquifers of the Khorat Group are generally confined (Buaphan et al., 1995). The gravels and sand of the Qt deposits are generally unconfined and the upper silt and sand of the Qa behaves as a confined aquifer due to confining clay layers (Buaphan et al., 1995; Löffler and Kubiniok, 1988). Qa aquifers are recharged primarily through precipitation (Williamson et al., 1989).

2.4.2 Capillary Rise

Soil and groundwater salinization is a result of the dissolution of weathered evaporative layers of the Mahasarakham Formation and mobilization of highly saline water by the processes of shallow interflow and capillary rise. These are the two main mechanisms for the formation of salinity in shallow soil and water, but there is disagreement regarding the degree to which each mechanism is responsible for distributing it. The first mechanism, suggests that shallow interflow, (or horizontal groundwater flow) through the unsaturated zone, is responsible for lateral transport of saline groundwater from the uplands to the lowlands. (Löffler and Kubiniok, 1988; Wongsomsak, 1986). The second proposed, suggests that the upward movement of groundwater in the unsaturated zone as a

result of cohesion, adhesion, and surface tension (Löffler and Kubiniok, 1988; Wongsomsak, 1986).

In unconfined aquifers, the water table is the boundary between the saturated and unsaturated aquifer zones. Above the water table, capillary force causes water to be pulled upward into the soil, a process known as capillary rise, creating an unevenly saturated feature known as the capillary fringe (Fetter, 2001). Grain size and shape determines the height of capillary rise and may be roughly estimated based on these characteristics (Table 1). The process of capillary rise is likely to play a key role in saline soil in the study area, specifically in areas where salt deposits are visible on the ground surface (Wongsomsak, 1986). Fine grain size and more pore space allows for more upward, or capillary, movement of saline groundwater. In fine-grained sediments that are characterized by silt and clay, capillary rise is slow, but water reaches greater heights than in coarser-grained material such as sand (Brouwer et al., 1985). Given the fine-textured sediments in the study area, capillary rise is expected to be between 0.015 m and several meters (Fetter, 1984).

Table 1 Estimated capillary rise heights of various sediment types (Brouwer et al., 1985; Fetter, 1994).

Sediment Type	Estimated Capillary Rise
Clay	80 cm (0.8 m) up to several meters
Fine silt	750 cm (7.5 m)
Coarse silt	300 cm (3 m)
Very fine sand	100 cm (1 m)
Fine sand	50 cm (0.5 m)
Medium- grained sediment	50- 80 cm (0.5- 0.8 m)
Coarse sand	15- 50 cm (0.15- 0.5 m)
Very coarse sand	4 cm (0.04 m)
Fine gravel	1.5 cm (0.015 m)

Although an influx of water would generally dilute salinity, increased precipitation and irrigation may actually increase soil salinity as a result of capillary rise. Seasonal precipitation variations affect the movement of saline water below the ground surface. The capillary process has been demonstrated to move saline groundwater upward into the unsaturated zone in response to cyclic water table fluctuations (Löffler and Kubiniok, 1988). At the beginning of the dry season, the water table is at its highest level, and evaporation and capillary rise cause an upward movement of saline water. The dry evaporative conditions cause the accumulation of precipitated salt in the unsaturated zone (Figure 2.7). Under the arid and evaporative conditions of the dry season, the water level and top of the capillary zone rise drop, and salts are left behind in the unsaturated zone (Löffler and Kubiniok, 1988; Wongsomsak, 1986). As the water table rises during the rainy season, saline ground water floods the pore spaces of the unsaturated zone, residual salts are dissolved, move upward, and accumulate at shallower depths as the capillary zone rises. As the pore water evaporates at the end of the rainy season and the water table drops, saline groundwater becomes concentrated, capillary rise occurs in the topsoil, and salt minerals precipitate. In extreme cases, the process results in the accumulation of salts as a crust on the land surface (Löffler and Kubiniok, 1988; Patcharapreecha et al., 1990).
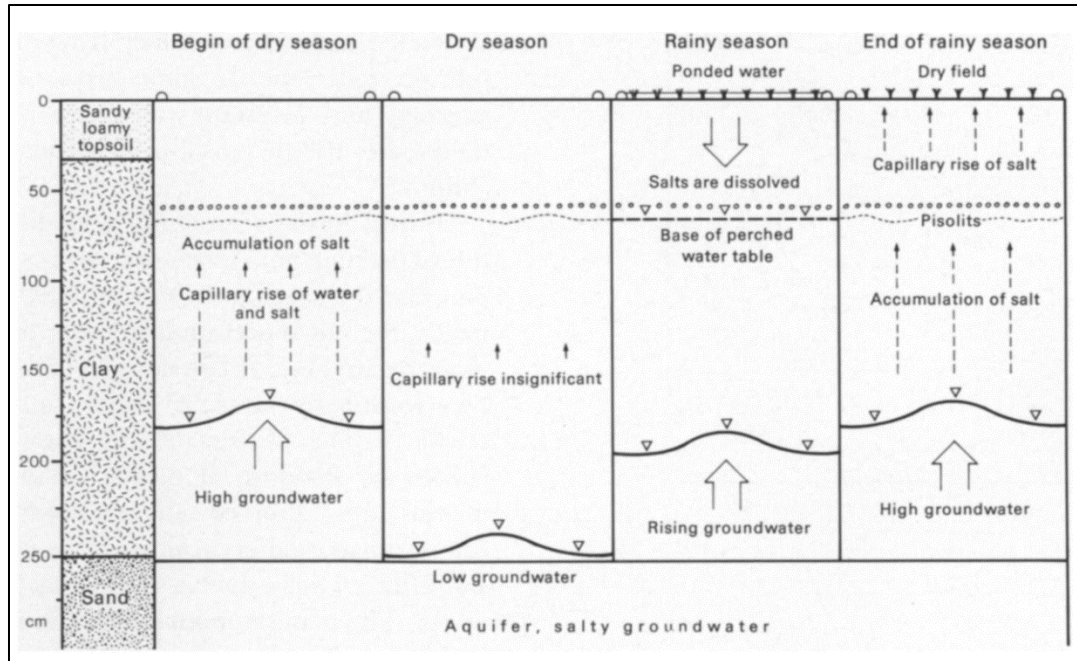
Figure 2.7 Capillary Rise in Saline Soils. Capillary rise begins at the start of the rainy season and increases with the amount of precipitation. As the water table rises, saline groundwater enters the topsoil (root zone) and accumulates in the unsaturated zone (Löffler and Kubiniok, 1988).

Wongsomsak (1986) states that the thickness of overlying sandy alluvium above salt-affected soil affects saline capillary rise in northeastern Thailand. Areas of greater alluvium thickness prevent salt precipitation from forming on the ground surface, even more effectively than upper clay layers (Wongsomsak, 1986). Likewise, Löffler and Kubiniok (1988) state that areas of sand lenses where clay is sparse are less prone to salinization.

2.4.3 Salinity, Electrical Conductivity, and Resistivity

According to the United States Geological Survey (USGS), fresh water is defined as having total dissolved solids (TDS) concentrations less than 1,000 parts per million (ppm), (U.S.G.S., 2021). Slightly saline water ranges from 1,000 to 3,000 ppm (2,000 to 6,000 µS/cm), moderately saline ranges from 3,000 to 10,000 ppm (6,000 to 20,000 µS/cm), and 10,000 to 35,000 ppm (20,000 to 70,000 µS/cm) is considered highly saline (U.S.G.S., 2021). Groundwater salinity in the Khon Kaen region has been observed to range from 200 to 88,000 µS/cm, where the lowest salinity is observed in Quaternary sand and gravel aquifers and the highest salinity occurs in Quaternary alluvium and Mahasarakham Formation aquifers (Srisuk, 1996; Wongsomsak, 1986).

The United States Environmental Protection Agency (2003) recommends drinking water with a maximum salinity of 20 ppm, or 40 µS/cm. High salt content in soil water can damage urban infrastructure such as roads, bridge supports, and building foundations, since saline water corrodes concrete structures (Cement Concrete & Aggregates Australia, 2018). Urban salinity has become a threat to an increasing amount of acreage in northeastern Thailand. In the city of Khon Kaen, within Khon Kaen Province, land use has changed dramatically over the past several decades and aggravated the salinity problem.

The electrical conductivity of a material is the degree to which an electrical charge moves through that material. A material with high electrical conductivity will have low electrical resistivity. Certain materials, such as clays, metallic minerals, and saltwater are

highly conductive. The conductivity/resistivity of subsurface can be used in geophysical studies to predict the lithologies of subsurface materials.

Since dissolved salt is electrically conductive it may be identified as low resistivity by ERT methods. Dissolved sodium chloride (NaCl) is the dominant salt in the soil and groundwater of the study area (Patcharapreecha et al., 1989; Srisuk, 1996). In fluids, conductivity measurements can be used to estimate salinity, based on a relationship between salinity and conductivity. If sodium chloride is assumed as the dominant dissolved ion in a solution it may be assumed that total dissolved solid (TDS) represent sodium chloride salinity. A relationship between TDS and electrical conductivity (EC) is given by the equation:

$$TDS\left(\frac{mg}{L}\right) = k \times EC\left(\frac{\mu S}{cm}\right)$$

where TDS units are mg per liter and EC units are µS/cm (Rusydi, 2017). The constant of proportionality, k, is dependent on the amount and the activity of ions in the solution (Rusydi, 2017). A study in the Lower Nam Kam River basin, approximately 200 km east of Khon Kaen, found k to be equal to 0.5 to 0.7 (Seeboonruang, 2013).

When water temperature is above 0° Celsius, the conductivity of water rises as temperature increases at a rate of 2 to 3% per degree (Miller et al., 1988). Specific conductivity (κ_s), is conductivity made at, or corrected for, a water sample at 25° C. Therefore, conductivity measurements obtained at temperatures other than 25° C need a correction using an equation similar to:

$$\kappa_s = \frac{\kappa}{1 + 0.02(T - 25)}$$

where κ_s = specific conductivity, κ = measured conductivity, T = temperature of the sample in degrees Celsius (Miller et al., 1988).

2.5 Climate

2.5.1 Temperature and Precipitation

Rainfall infiltration is an important source of aquifer recharge in the region (Wongsawat et al., 1992). Northeast within tropical latitudes, so the region has a warm and seasonally wet climate (Thailand Meteorological Department, 2015). Seasonal monsoon winds control Thailand's climate. The northeast experiences 66% to 69% humidity and an average of 116 rainy days per year, based on data collected from 1981 to 2010 (Thailand Meteorological Department, 2015). Northeastern Thailand experiences three main seasons: pre-monsoon season (summer), southwest monsoon season (rainy), and a northeast monsoon season (winter) (Thailand Meteorological Department, 2015). Summer lasts from mid-February to mid-May, the rainy season from mid-May to mid-October, and winter from mid-October to mid-February (Thailand Meteorological Department, 2015).

Mean temperatures in the northeast are 28.6°C in the summer, 27.6°C in the rainy season, and 24.2°C in the winter (Thailand Meteorological Department, 2015). The hottest months of the year occur during the summer, from March to May, when temperatures may

exceed 40°C. Approximately 224.4 mm of precipitation occurs during the summers (Thailand Meteorological Department, 2015). The rainy, or southwest monsoon season, is typically frequented by thunderstorms and dropping temperatures (Thailand Meteorological Department, 2015). The rainy season may include several weeks of scarce rainfall yet averages 1,103 mm of seasonal precipitation (Thailand Meteorological Department, 2015). Winter, or northeast monsoon season, is dry and typically mild but can be cold, reaching temperatures as low as 0°C, in December and January. Winter has an average precipitation of 76.3 mm, but some months see zero rainfall (Thailand Meteorological Department, 2015).

In recent years, the rainiest months appear to be occurring later than in the past. Ten-year average rainfall amounts were determined for each month of the year, using data from the Khon Kaen airport meteorological station (Figure 2.8). In 2019 and 2020, the pattern of monthly rainfall matched those of the ten-year average, but monthly amounts differed (Figure 2.8). Precipitation levels were much higher than average in May of 2019 when most of the data for this study was collected. September 2019 precipitation was also higher than average, but lower than average in June, July, August, and October. In 2020, no precipitation fell in January, February, and December. April 2020 precipitation was lower than average, while March, September, and October precipitation was much higher than average.

Figure 2.8 Precipitation in Khon Kaen, Thailand. The blue bars represent the 10-year monthly precipitation average at the Khon Kaen airport meteorological station (timeanddate.com). The dark blue and light blue lines depict monthly rainfall measurements in 2019 and 2020, respectively, and were recorded at the Khon Kaen airport meteorological station by the Thailand Meteorological Department (2019- 2020).

Precipitation is expected to dilute saline water in closed systems of water. However, in areas with seasonal processes of wetting and drying, along with vertical water movement, results may differ. As water evaporates from the ground surface salt solids are left behind and may affect water salinity when dissolved by precipitation.

2.5.2 Drought

Thailand is becoming increasingly affected by drought due to climate change and

El Niño weather patterns (Marks, 2019). Between 1988 and 1992, Thailand's water resource volume was an average of 3.9 million cubic meters, but this volume dropped 18% to an average of 3.3 million cubic meters between 2013 and 2017 (Marks, 2019). When drought occurs, there is less recharge to the aquifers.

Thailand also experienced extreme droughts in 2015 and 2016. Precipitation in 2015 was 46% below normal levels and reservoir capacity was at 45%. These droughts impacted Khon Kaen harshly (Marks, 2019). The Ubol Ratana Dam, northwest of the city of Khon Kaen, dams the reservoir holding the city's water. The water level in June 2015 was at 10% of its capacity (Marks, 2019). Farmers were severely impacted by the shortage and barred from growing a second crop, however, industrial residential tap water use was not restricted (Marks, 2019). In 2019, the monsoon rains were five weeks shorter than normal, and an El Niño event led to high temperatures and subsequent high evapotranspiration (Marks, 2019). These conditions led to a drought in 2020 which was the most extreme in Thailand in 40 years (Dauphin and Patel, 2020).

Thailand's extreme drought in the beginning of 2020 is visible in a subsurface soil anomaly map, which depicts how far the amount of water near the ground surface is from the normal amount (Figure 2.9). The map is based on satellite data collected from a radiometer that analyzes moisture content in the upper 5 cm of soil. All of Thailand is light to dark brown because the entire country received much less precipitation than normal (Figure 2.9). As climate change exacerbates drought conditions, the most vulnerable populations will face greater threats and increasing drought conditions place even more

importance on understanding groundwater conditions and water resource management.
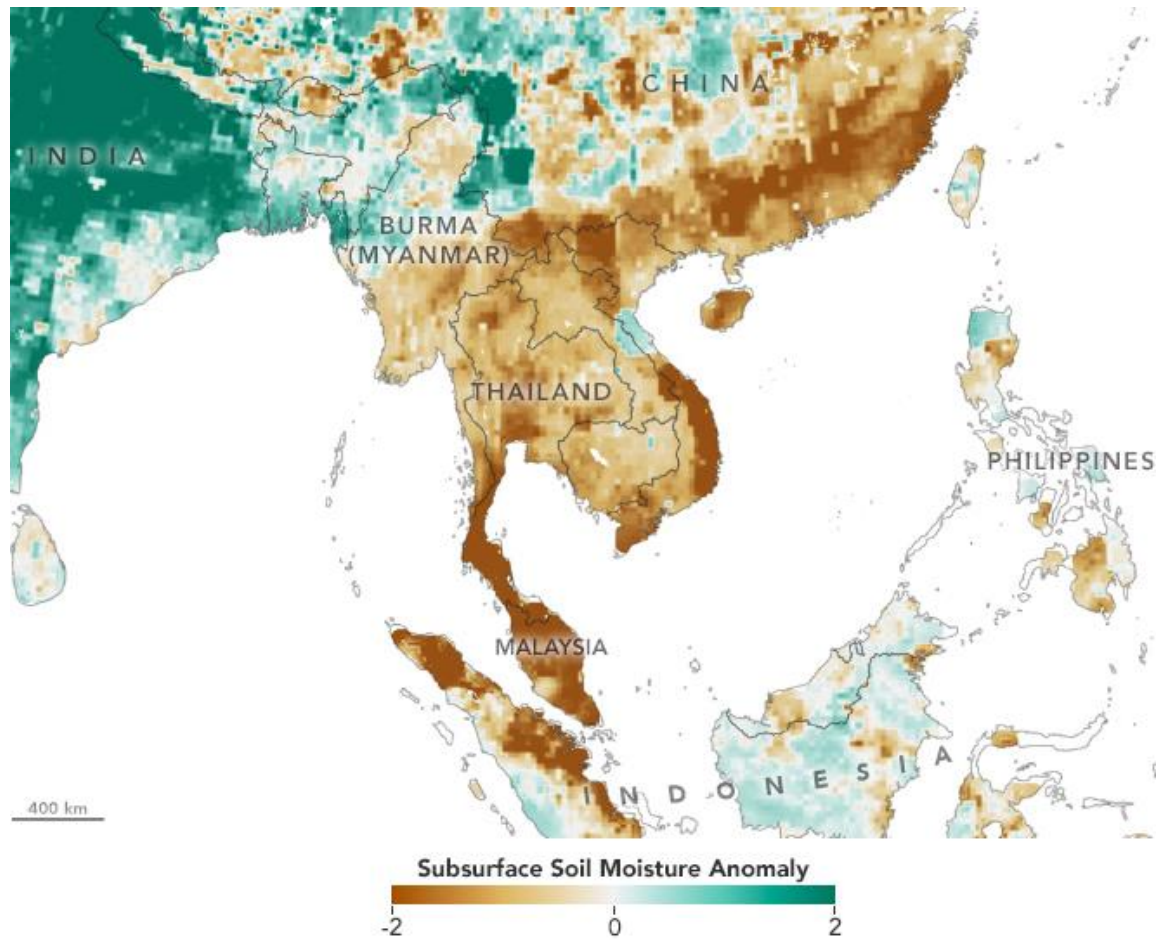
Figure 2.9 NASA Earth Observatory subsurface soil moisture anomaly image using soil moisture data from NASA, USDA, and the SMAP Science Team (Dauphin and Patel, 2020).

2.6 Electrical Resistivity Tomography (ERT)

Conventional techniques used in groundwater studies, such as well drilling and borehole geophysics, provide one dimensional information specific to the well location. Geophysical techniques utilizing electrical resistivity provide at least two-dimensional data along a profile and are efficient in terms of cost and time (Riwayat, Nazri, and Abidin, 2018). Many studies of seawater intrusion have utilized ERT surveys to identify the presence of saline groundwater and to define fresh and saltwater boundaries (Galazoulas et al., 2015; Jansen, 2011; Riwayat et al., 2018). This method is also now used for dryland salinity, defined as continental soil and groundwater salinity, in Australia (Foley et al., 2012). Recently, Arjwech et al. (2020) have evaluated the use of ERT in a study of saline groundwater in the Khon Kaen region.

Electrical resistivity tomography (ERT) is a low-cost, non-destructive, near-surface geophysical technique that measures material resistivity. ERT is used for a variety of subsurface exploration, including ore deposits, faults, void spaces, groundwater, contamination, and geologic structures (Burger et al., 2006). Various materials respond to applied currents differently, with the same material having a wide range of possible resistivity values (Figure 2.10). ERT identifies variations in subsurface materials and structures by measuring their response to current. Resistivity is determined by measuring the amount of voltage allowed to travel between the two points (Burger et al., 2006). The electrodes may be configured into different geometries depending on the survey goals. In a Wenner-Schlumberger array, the electrodes are inserted an equal distance apart and left in place during data collection.
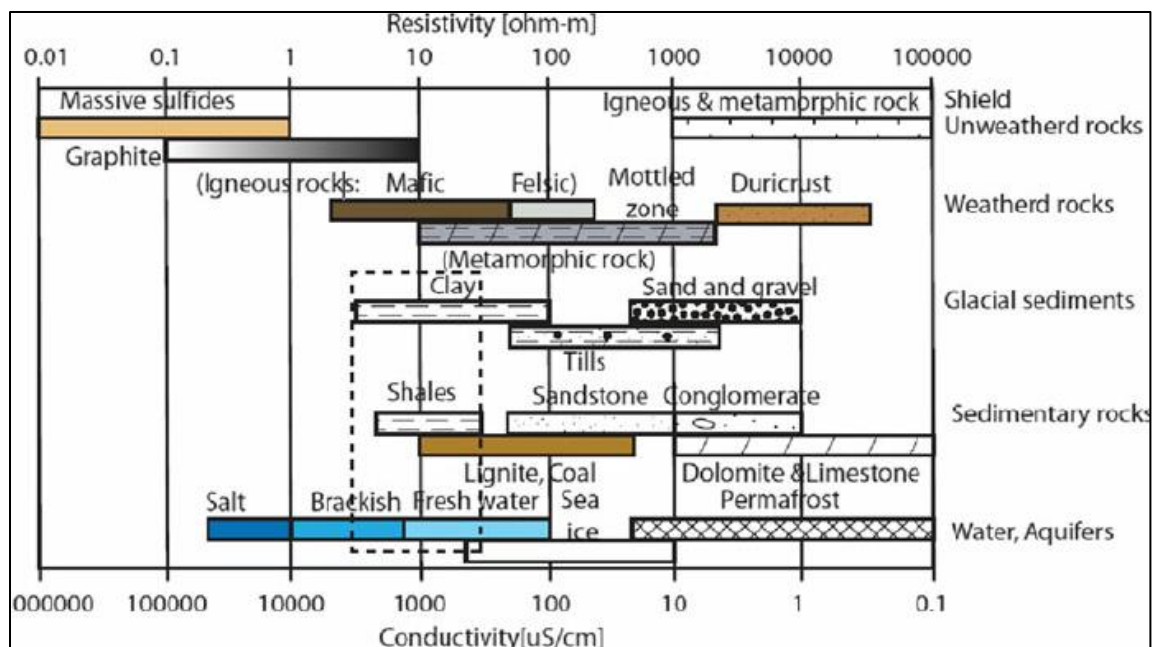
Figure 2.10 Typical range of resistivities for common geologic materials (Sikandar and Christen, 2012).

Since saline water is more conductive than fresh water, ideally, an ERT survey may indicate locations along the profile line of underground water and soil that are more saline than other areas. However, resistivity values are also influenced by clay minerals and water content (Arjwech et al., 2020). Further, lithified materials may have a wide range of possible resistivity values, as a result of the degree of weathering or fracturing. Typically, compaction and lithification, and coarser grain sizes result in higher resistivity values for a given rock type (Burger et al., 2006). Generally, saturated sediments have lower resistivity than underlying bedrock in freshwater conditions (Burger et al., 2006). Briški (2020) reported that saturation may affect the resistivity of the same rock from 100 to 1,000,000 ohm-meters. When the material is saturated, the degree of porosity, fracturing, and weathering may contribute to lower resistivity values (Burger et al., 2006).

Nevertheless, Burger et al. (2006) recommend that the only way to have complete confidence in interpreting geologic conditions based on resistivity data is by comparing lithologic descriptions from drilling logs to an ERT profile.

The configuration of an ERT survey is analogous to an electrical circuit. Since current flows from positive to negative electrodes, and the current source is positive, the current flows towards a current sink which is negative (Figure 2.11). In an ERT survey, a transmitter introduces current into the ground and measures the potential difference between two points at the surface. The potential difference, or voltage, is the amount of current that flows between the potential electrodes and is determined by subtracting the potential at a second location from that of a first location. The resistivity (ρ) of the subsurface material is calculated from these measurements using the equation

$$\rho = \frac{2\pi\Delta V}{i} \left(\frac{1}{\frac{1}{r_1} - \frac{1}{r_2} - \frac{1}{r_3} + \frac{1}{r_4}} \right)$$

where ΔV = the voltage difference between P_1 and P_2 (in volts), i = the amount of current (in amperes) applied at C_1, r_1 = the distance between C_1 and P_1, r_2 = the distance between P_1 and C_2, r_3 = the distance between C_1 and P_2, and r_4 = the distance between P_2 and C_2 (all distances in meters) (Burger et al., 2006).
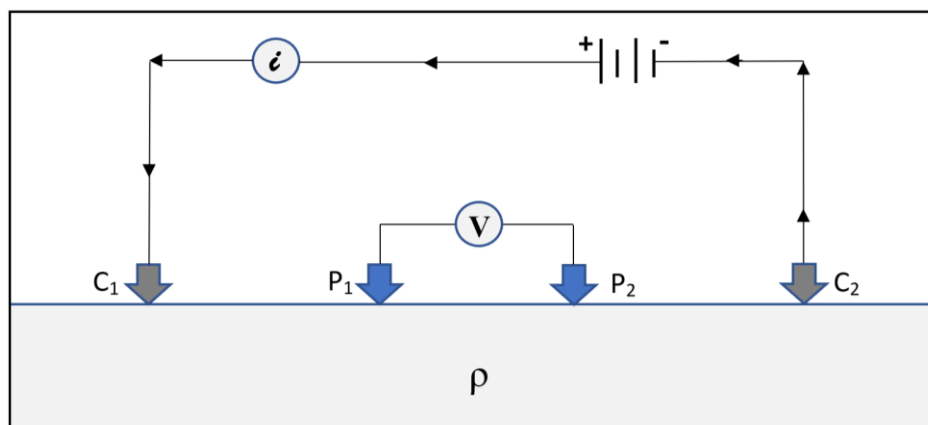
Figure 2.11 Electrical resistivity survey configuration. C_1 and C_2 are where current is introduced. C_1 is the positive current electrode, C_2 is the negative current electrode. P_1 and P_2 are the potential electrodes, between which the potential difference is measured. (Adapted from Burger et al., 2006).

An ERT survey requires a resistivity meter, containing a transmitter and a receiver, an external 12-volt battery, stainless-steel stakes, electric cables with embedded coiled metal (electrodes), measuring tapes, and a laptop with specific software. The stainless-steel stakes are inserted into the ground along the profile at 5 m increments and attached to the electrodes with metal clips and coated wire. Ideally, GPS and elevation data are collected along the profile using survey equipment, such as a theodolite, to accurately determine depth. Since the field-acquired data is a sum of all of the subsurface resistivities at all depths, the raw data requires post-survey processing. This process includes apparent resistivity calculations and an inversion to estimate how the resistivity is truly distributed in the subsurface (Burger et al., 2006). A processed ERT profile appears as a spectrum of color that represents a spectrum of resistivity values (Figure 2.12).
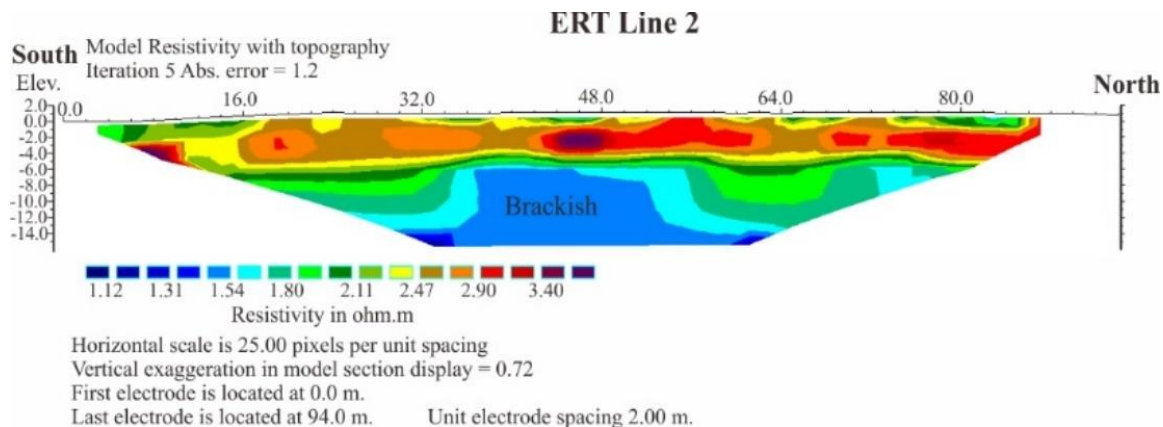
Figure 2.12 An example of a processed ERT profile. The lowest resistivity areas are dark blue, and the highest are red and dark purple (Arjwech et al., 2020).

2.7 Other Work

In an ideal study with unlimited resources, geologic and hydrochemical information from well logs and water samples and borehole geophysical logs would be used to define areas of fresh, brackish, and saline groundwater (Williams and Spechler, 2011). However, other methods are needed when well drilling and borehole logging are not practical. For instance, wells cannot be drilled everywhere due to cost and accessibility, analysis of lateral geologic differences becomes complicated even with numerous wells, and borehole logging may not be available and is well-specific. Research that combines more than one method forms a more complete understanding of subsurface conditions.

Greggio et al. (2018) found that ERT, combined with groundwater and water level data, was effective in locating essential freshwater lenses with consistent and reproducible results in their study of a coastal, salinized aquifer in Ravenna, Italy. The authors

determined ERT to be a quick method of understanding and managing sparse water resources as they change over time, when combined and correlated with data from boreholes, piezometers, and groundwater sampling (Greggio et al., 2018). At this site, the material is entirely well-sorted medium to coarse grained sand, therefore, the variation in ERT resistivity values could be attributed solely to differences in saturation and salinity (Greggio et al., 2018). Using the combined data, four distinct areas of resistivity defined the locations of the unsaturated zone, capillary fringe, water table, freshwater, and brackish-saline groundwater (Greggio et al., 2018).

Najib et al. (2017), conducted a study in which major ion analysis of groundwater collected from 46 wells was compared to results from 10 ERT lines to identify the location and extent of salinization of a coastal, unconfined aquifer in Chaouia, Morocco. Previous research concluded that salinity in the aquifer was a result of overpumping, fertilizers, sea spray, recycling irrigation water, evaporation, ion exchange, water-rock interaction, and seawater intrusion, and this study intended to clarify the mineralization source (Najib et al., 2017). The groundwater level in this study area is between -0.2 and 0.6 mamsl and the authors recommend at least one-meter electrode spacing in similar environments to ensure accurate results with shallow water table levels (Najib et al., 2017). The study found that the main source of salinity is seawater intrusion and significantly, that out of 23 auger holes tested for conductivity, 18 had chemistry data verified by the ERT resistivity data and five that did not (Najib et al., 2017).

Galazoulas et al. (2015) effectively used geophysics and hydrogeology to model a

coastal aquifer undergoing seawater intrusion in northeastern Greece. This study combined 12 ERT lines covering 15 km, 28 lithological logs, 31 groundwater quality samples, and 5 gamma ray logs (Galazoulas et al., 2015). The geology is well-known and includes unconsolidated alluvial and lacustrine sediments, including gravel, sand, silt, and clay, specifically a distinctive green plastic clay used as a marker between aquifers (Galazoulas et al., 2015). The distinguishing aspect of this study is the model the authors created, which includes data from each of the methods. The model integrates the gamma ray logs and lithologic columns superimposed on the ERT profiles, connecting lithology and resistivity in a visual manner. The diagrams also incorporate proposed aquifer boundaries, water table levels, and seasonal conductivity measurements at well locations on the profile, noting the wells' distance away from the ERT line (Galazoulas et al., 2015). The fusion of methods allowed the authors to successfully define aquifer geometry and boundaries, determine where recharge occurs, and delineate the interface between fresh and saline water (Galazoulas et al., 2015).

Arjwech, Everett, and Schulmeister (2019) utilized ERT in combination with vertical electrical sounding (VES) and historical salinity data in the City of Khon Kaen and on the Khon Kaen University campus to identify areas of soil salinity. The data from individual geophysical and hydrological methods, such as ERT and water conductivity testing, provided a more complete understanding of the subsurface. Their results suggest that near the University, saline porewater is at shallow depths in the floodplains and at deeper depths in higher, hilly areas (Arjwech et al., 2020).

CHAPTER 3

METHODS

3.1 Study Design

This thesis tested the hypothesis that electrical resistivity tomography (ERT) can be used to identify the top of the water table in fresh-water aquifers and the top of the capillary zone in saline aquifers. To investigate, ERT results, groundwater conductivities, water level measurements, and lithologies were compared in locations where fresh, brackish, and saline groundwater occur. Groundwater samples from wells adjacent to ERT profiles were used to obtain water table and groundwater salinity information. Further, the relationship between seasonal variations in the water table, groundwater chemistry, and the ERT results were compared. To evaluate the possible seasonal variations in water salinity, measurements were made during both the dry and rainy seasons from all accessible wells within the study area. Soil and groundwater chemistry and ERT results were used to evaluate salinity conditions.

Seventeen wells were located in the study area for which the Thailand Department of Groundwater Resources maintained well logs as part of their database (Table 2). The well information included location data in easting and northing coordinates using the Universal Transverse Mercator system and for some wells, drilled depth and screened interval depth measurements. Screened sections are used in some water wells to filter, allow water to flow out, and maintain the integrity of the well. Of the 17 wells used, water

levels were measured in 14 of the wells that could be accessed without dismantling the well's casing or removing its pump. Water samples were collected from all 17 wells, although some water samples were only obtainable from a port next to the well. The water table elevation at each well was calculated by subtracting the water depth measurement from ground elevation at the well. Land surface elevations were obtained from GPS Waypoints Mobile Application (Bluecover Location Based Technology, 2019). The wells are ordered from west to east.

Table 2 Well locations and construction parameters used in this study (Thailand Department of Groundwater Resources, 2019). NA indicates no available information. Wells denoted with an asterisk (*) were sampled via a port.

WELL NAME	EASTING (m)	NORTHING (m)	ELEVATION (m)	DRILLED WELL DEPTH (m)	SCREENED INTERVAL (m)
S1710	252127	1824872	188	72	12-18, 42-48, 66-72
S1735	254075	1822957	178	48	28-32
F471	254408	1822496	179	46.5	28.5-34.5
Y948	254529	1821968	181	49	36-48
KK101	256825	1820277	177	26	NA
F1599	258418	1825657	174	24	20-24
DP421	260526	1822831	172	32	24-30
F1600	260673	1822222	176	24	20-24
F1593	260698	1822215	178	24	NA
KK91	260727	1822244	177	29	NA
DP465*	260719	1822820	177	53	45-51
RTB174*	261448	1823047	213	84	74-80
TX210	266122	1822362	190	58	48-54
F186	266320	1821080	170	81	58.5-76.5
Y1905	266473	1821910	173	50	37-46
S1863	266581	1821909	181	54	40-49, 50-53
F823	268496	1821638	169	21	15-21

Water levels were measured, and samples were tested for conductivity at the beginning and the end of the rainy season so that the impact of seasonal salinity variations on groundwater salinity, groundwater levels, and ERT profiles could be compared. Attempts were made to measure specific conductance and water level three times per season, to identify water table the degree of fluctuation that may occur at each site. In most cases, three measurements were not possible due to the influence of intermittent well use and pumping on ground water levels or well inaccessibility. Each well was sampled as many times as possible and the average of each set of seasonal measurements was used as a seasonal value.

3.2 Methods and Equipment

3.2.1. Determination of the Site Stratigraphic Framework

Since resistivity values provided by ERT surveys values depend on lithology, specifically clay content, as well as water presence and mineral content, ERT data interpretation requires background knowledge of the study area geology. Prior to conducting field work, the subsurface stratigraphy of the study area was mapped using drillers logs available at the Thailand Department of Groundwater Resources online database and published reports (Thailand Department of Groundwater Resources, 2019). Geologic cross-sections were constructed using lithologic logs for existing domestic and monitoring wells.

3.2.2 Geologic and Groundwater Maps

Seventeen wells were chosen for this study based on their locations and accessibility. One set of wells was chosen that are located primarily in Quaternary alluvium and another in the Quaternary terrace deposits. The lithologic logs display an extremely variable lateral change in lithology and many interbedded layers. The lithologic descriptions from study area and nearby wells include various colors and combinations of clay, sand, gravel, shale, and minor laterite beds and lateritic soils (Thailand Department of Groundwater Resources, 2019). A personal computer and software including Microsoft Office, Google Earth, and QGIS with various plugins were used.

3.2.3. Groundwater Sampling

Areas of high soil and groundwater salinity were identified based on sampling in 17 domestic and irrigation wells. Samples were extracted from the wells using a metal water bailer after three to five bailer volumes were removed (Figure 3.1). Conductivity, pH, and temperature were measured in the field using handheld conductivity and pH meters, which were rinsed twice prior to sample collection (Figure 3.2). Conductivity values were auto adjusted for temperature (25 degrees C) and reported as specific conductance, although the term Conductivity is used throughout this thesis. The use of two instruments, an Oakton PCSTestr 35 (Oakton, 2010) and a Hanna H198121 (Hanna, 2019), allowed for the verification of an instrument's potential drift by comparing readings of both instruments throughout each sampling event. A potassium chloride standard with a

concentration of 0.7459 g/L and pH 4 and pH 7 buffer solutions were used to calibrate the

conductivity and pH of the pH/salinity meters were required. Although pH data was not

used in this analysis, it was measured as an accessary parameter and the results are included

in Appendix B. Other necessary laboratory equipment included distilled water, plastic

sampling bottles, plastic beakers, glass beakers, and an Erlenmeyer flask.

Figure 3.1 Gathering a water sample with water bailer. Photo by Dr. Marcia Schulmeister.

Figure 3.2 Measuring conductivity with a handheld salinity meter. Photo by Dr. Marcia Schulmeister.

Groundwater levels were measured in 14 wells using an electric sounding tape (Figure 3.3). Well depths range from 21 to 81 meters deep and are finished in the unconsolidated Quaternary deposits and the upper part of the Phu Tok Formation. Water levels were measured at the beginning and the end of the rainy season to compare the impact of seasonal salinity variations on groundwater salinity and groundwater levels.

Figure 3.3 Measuring depth to water in a domestic water well with an electronic tape measure. Photo by Dr. Marcia Schulmeister.

3.2.4 ERT Profiles

The equipment required to conduct an ERT surveys includes: a resistivity meter, laptop, cables, electrodes, metal stakes, surveying (elevation) tripod equipment, and multiple tape measures (Figure 3.4). This study used a Syscal R1 Plus multi-electrode imaging system, with 200 W of power and 600 V voltage, to obtain resistivity data (Syscal, 2020). The Syscal resistivity meter is connected to electrodes, which are connected to metal stakes inserted into the ground. Two surveys were conducted, with lines 235 and 400 meters long, each with 47 and 84 electrodes and 5-meter spacing, respectively, using a Wenner-Schlumberger array (Figure 3.5).

Figure 3.4 ERT survey equipment includes: a resistivity meter, laptop, cables, electrodes, metal stakes, and multiple tape measures. Photo by Romyupa Srikraiwest.

Figure 3.5 Left (top): cable attached to wire, attached to stainless-steel stake that is inserted into the ground. Left (bottom): ERT electrode. Right: laying ERT survey cable out along the profile. Left photos by Dr. Marcia Schulmeister, right photo by Romyupa Srikraiwest.

CHAPTER 4

RESULTS

4.1 Interpretation of Lithologic Logs

Ten of the wells in the study area that were available for groundwater measurements also had associated lithologic logs (Figure 4.1). Based on interpretation of the logs, geologic units include topsoil, laterite, clay, sand, gravel, and shale. The study area hosts complex stratigraphy that varies laterally most likely as a result of its history of fluctuating river environments. A case in point is the high degree of lateral lithologic variation apparent between wells F1600 and F1593. The two wells are approximately 25 meters from each other and vary considerably in stratigraphy. In the lithologic logs, well F1600 is described as having 5 meters of topsoil underlain by a clay layer at least 19 meters thick. A short distance of 25 meters away, a topsoil description is absent for well F1593, described only as having a 6-meter-thick upper clay layer with underlying shale at least 12 meters thick.

Many of the logs are incomplete and contain only partial notes. Irregularities in the lithologic descriptions may be due to file format error, mistranslation, or simply individual differences in lithology interpretations made by the geologist. For example, the lowest layer of well 1600 is described as "brown clay" under a layer labelled, simply, "clay." Another example of a possible inconsistency in geologic identification is in well S1710, where more than thirty meters of shale appear to overlie a layer of shale and clay. Shale is a sedimentary rock and clay is a sediment that has not been lithified. Sediment does not

usually exist below sedimentary rock in an area that has not experienced extreme structural deformation. Perhaps the labels clay and shale were used interchangeably, or the clay is in fact shale or claystone. Given the region's dramatic fluvial history, the possibility exists that there is considerable lateral variation within a drilled well itself and the logs are accurate. While these lithologic logs were helpful in terms of developing a general understanding of local geology, further investigation and identification of site-specific lithology will be helpful to future projects.
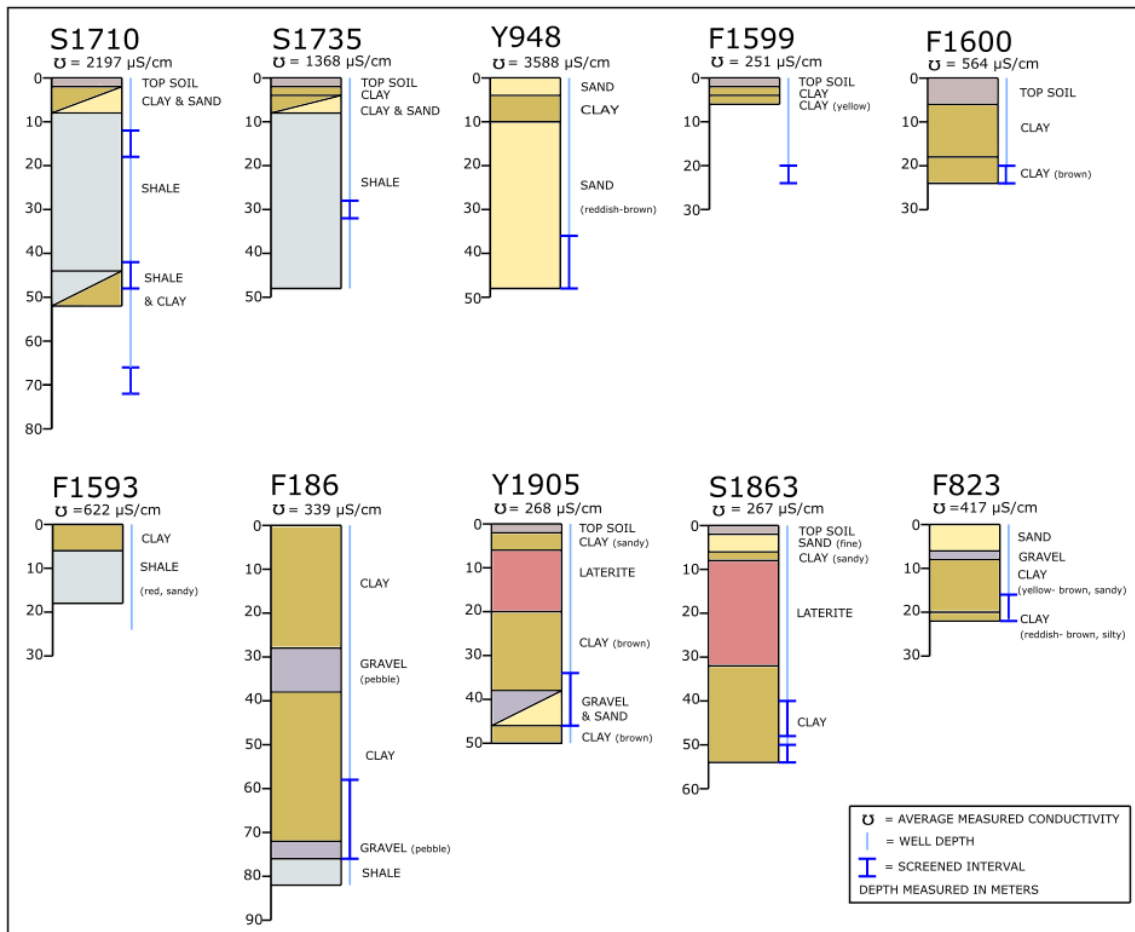
Figure 4.1 Drillers logs for study wells depicting the lithology of tested wells (Adapted from Thailand's Department of Groundwater Resources).

4.2 Geologic Cross Sections

Based on the lithologic logs, three geologic cross sections of the study area were constructed to provide information to support resistivity survey interpretation and discern conductivity/salinity patterns (Figure 4.2). The length of cross section A- A' is 20.0 km, cross section B-B' is 12.5 km, and cross section C-C' is 12.0 km. All the labelled wells had

lithologic logs available from Thailand's Department of Groundwater Resources. The wells with blue markers were sampled as part of this study. The wells with red markers had associated lithologic logs and were used to construct the cross sections; however, these wells are now covered and inaccessible. Cross sections were created using Inkscape Project software (2020).
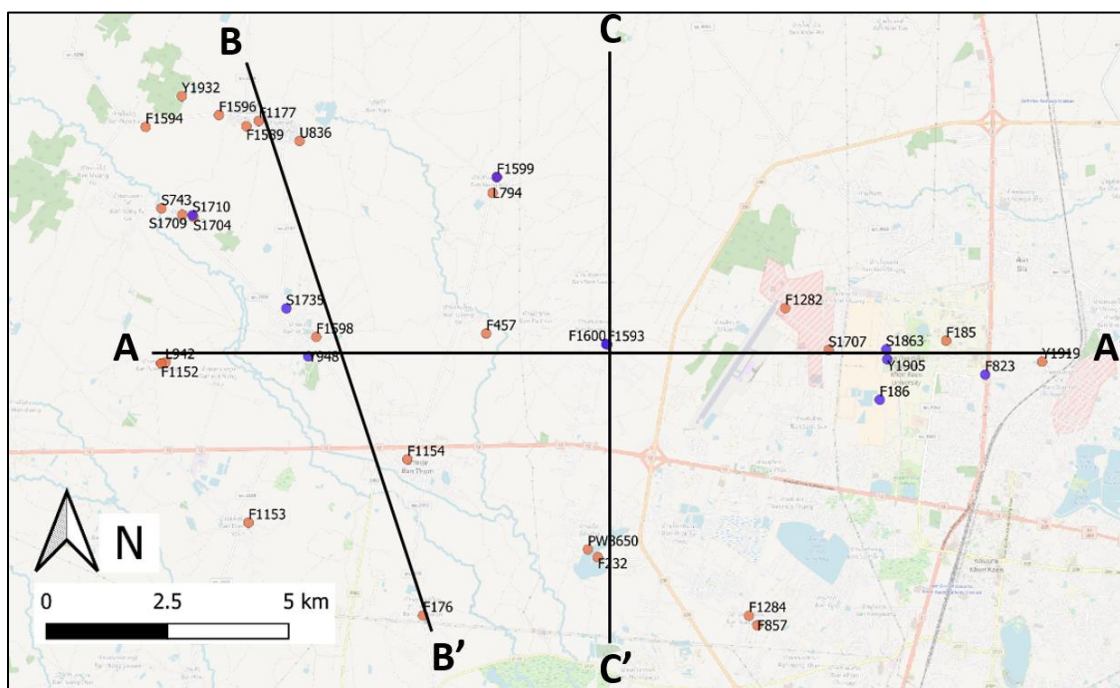
Figure 4.2 Geologic Cross Section Locations. The labelled points are wells with available lithologic logs used to make the cross sections. Blue markers indicate accessible wells sampled for measurement of groundwater conductivity in this study. Red markers indicate inaccessible wells, for which lithologic logs were available

Cross Section A-A'

Geologic cross section A-A' runs west of the city to close to the center of the city of Khon Kaen (Figure 4.2). On this cross section, wells sampled for conductivity are labelled, and the drilled depth is indicated by a blue line (Figure 4.3). The lateral geologic variations are apparent. The interbedded shale and sandstone lenses form the bedrock of the region. The unconsolidated gravel, sand, and clays represent Quaternary deposits. Clays are yellow, gray, brown, and red-brown and may be mixed with sand or gravel. Laterite is present. The Quaternary deposits in the east represent terrace deposition. Wells appear to be finished in all lithologies, including sandy clay.
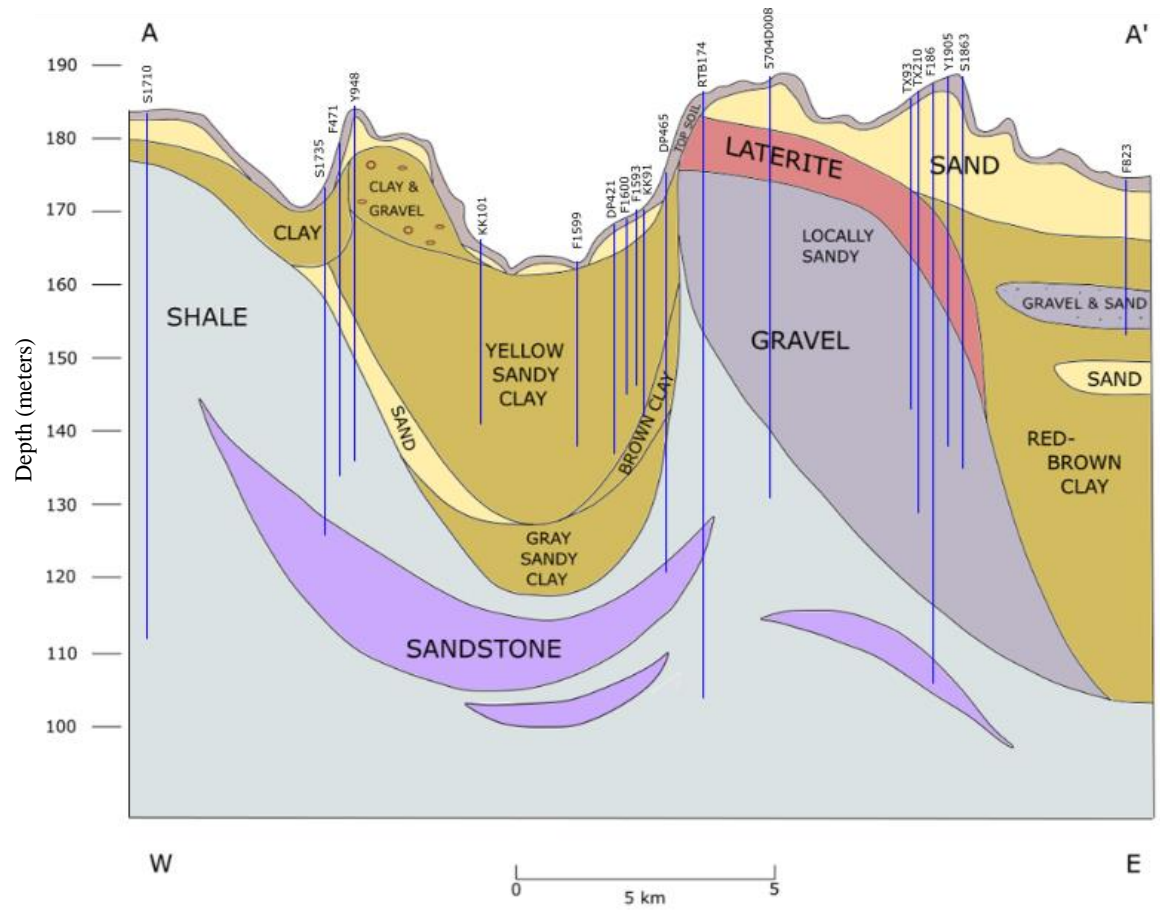
Figure 4.3 Geologic Cross Section A-A' from west to east across the city of Khon Kaen (See Figure 4.2). Well locations and depths, and lithologic logs were obtained from Thailand's Department of Groundwater Resources.

Cross Section B-B'

The geologic cross section B-B' is oriented north to south and is located west of the city of Khon Kaen. Wells tested in this study are labelled, and the drilled depth is indicated by a blue line (Figure 4.4). The northern region of the study area is more geologically complex, with interbedded layers of laterite, various clays, sand, and sand and gravel. Clay layers differ in color consisting of brown, white, or yellow varieties. Shale and sandstone form the bedrock and is overlain solely by sand in the southern part of the region. Wells appear to be finished in shale and sandstone only.
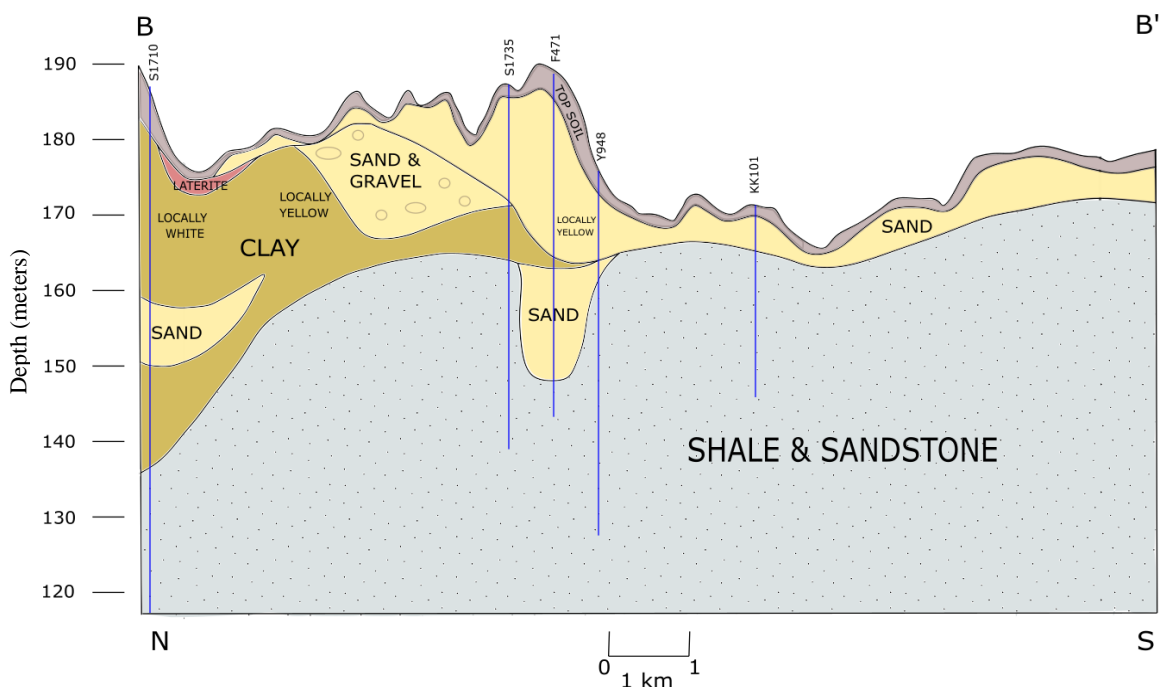
Figure 4.4 Geologic Cross Section B-B' (See figure 4.2). Well locations and depths, and lithologic logs were obtained from Thailand's Department of Groundwater Resources.

Cross Section C-C'

Geologic cross section C-C' extends from north to south and is located west of the city of Khon Kaen and is east of cross section B-B'. Tested wells are labelled, and the drilled depth is indicated by a blue line (Figure 4.5). This cross section displays mostly clay, with some sand, above shale and sandstone bedrock. To the south, there is an alternating pattern of clay and sand, with minor gravel above the shale and sandstone. Wells appear to be finished in sandy clay, sand, and the shale and sandstone bedrock.
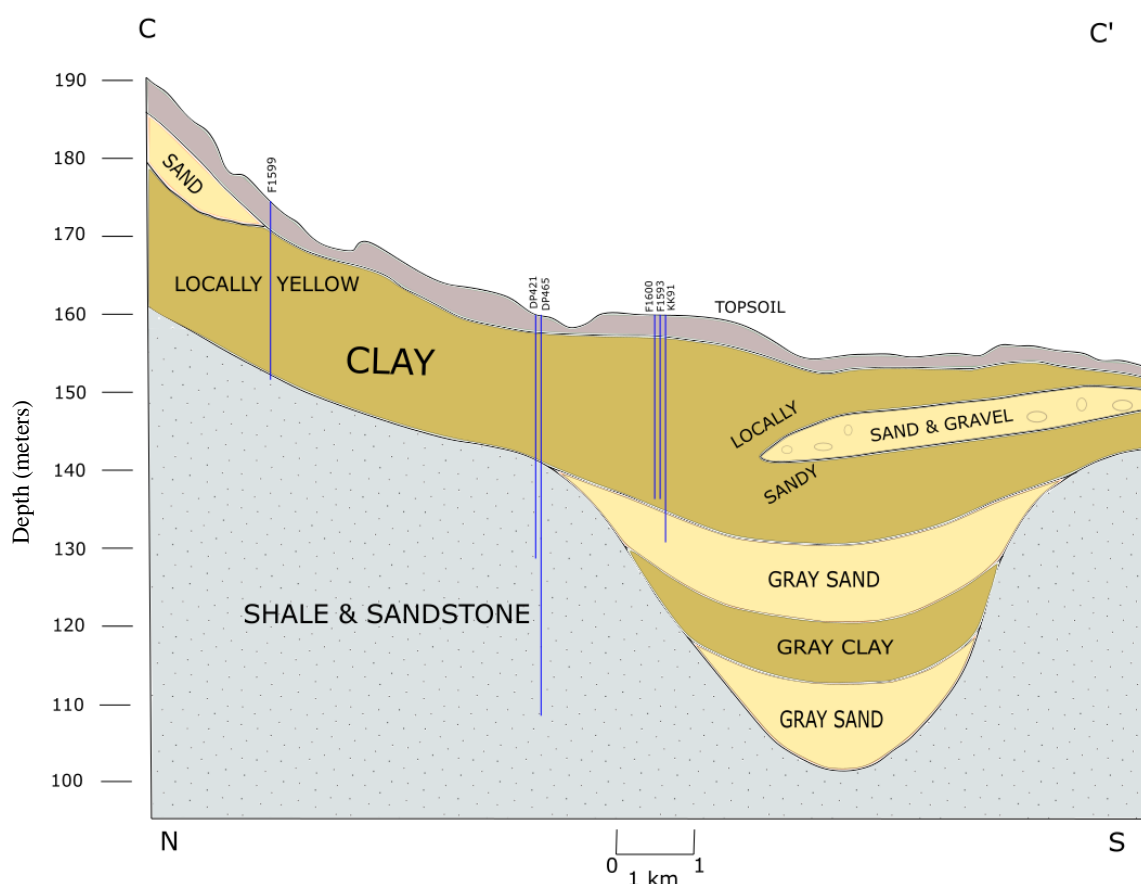
Figure 4.5 Geologic Cross Section C-C'. (See figure 4.2). Well locations and depths, and lithologic logs were obtained from Thailand's Department of Groundwater Resources.

4.3 Groundwater Wells and Water Chemistry

According to the U.S.G.S. (2021) designations for water salinity, the groundwater in the seventeen wells tested for conductivity in this research is considered fresh, slightly saline, and moderately saline (Table 3). Among these, fourteen of the wells are considered fresh. Two wells are considered slightly saline, and one is moderately saline. The twelve freshest wells are the most eastern of all the wells.

Table 3 Average groundwater conductivity and water levels during dry and rainy seasons. NA indicates no available information because the well was inaccessible. Wells denoted with an asterisk (*) were sampled via a port.

WELL NAME	AVERAGE CONDUCTIVITY (uS/cm), RAINY SEASON	AVERAGE CONDUCTIVITY (uS/cm), DRY SEASON	AVERAGE WATER TABLE ELEVATION (mamsl), RAINY SEASON	AVERAGE WATER TABLE ELEVATION (mamsl), DRY SEASON
S1710	2197	2105	181	172
S1735	1368	1353	168	155
F471	1678	1499	170	159
Y948	3588	NA	171	NA
KK101	6458	6580	172	169
F1599	251	426	172	169
DP421	118	117	170	166
F1600	564	526	171	165
F1593	699	673	NA	NA
KK91	381	342	172	168
DP465*	282	158	NA	NA
RTB174*	288	293	NA	NA
TX210	220	242	179	167
F186	339	309	167	165
Y1905	268	267	166	158
S1863	267	261	172	162
F823	417	404	167	NA

Seasonal Differences in Fluid Conductivity Across the Site

Well Y948 has the second highest conductivity measurements and was closed between the rainy and dry seasons. Higher fluid conductivity was observed in the western part of the study area during both seasons (Table 3). Seasonal fluctuations in salinity occur in parts of the study area, with higher conductivity observed during the rainy season in most wells (Figure 4.6). The rainy season average conductivities ranged from 118 to 6458 µS/cm and between 117 and 6580 µS/cm in the dry season. The difference between the average rainy and dry season conductivity measurements is between 1 and 179 µS/cm. Twelve out of sixteen wells had higher conductivity values during the rainy season. Salt accumulation in the unsaturated zone as a result of capillary rise and its subsequent dissolution as the water table rises may account for higher conductivity values during the rainy season.

Specific conductance differed between the rainy and dry seasons by 34 µS/cm and 97 µS/cm at the Bannonglub site and Ban Muang site, respectively. Despite the wells in this study classified as, at most, moderately saline, all but one of the tested wells are still open, and most are still in use. The wells that have been closed may host more saline groundwater. Wells that have been closed may no longer be needed, or perhaps the water was too saline for consumption. All the tested wells had conductivity measurements beyond the EPA's suggested maximum salinity, at least for taste and low-sodium diets.
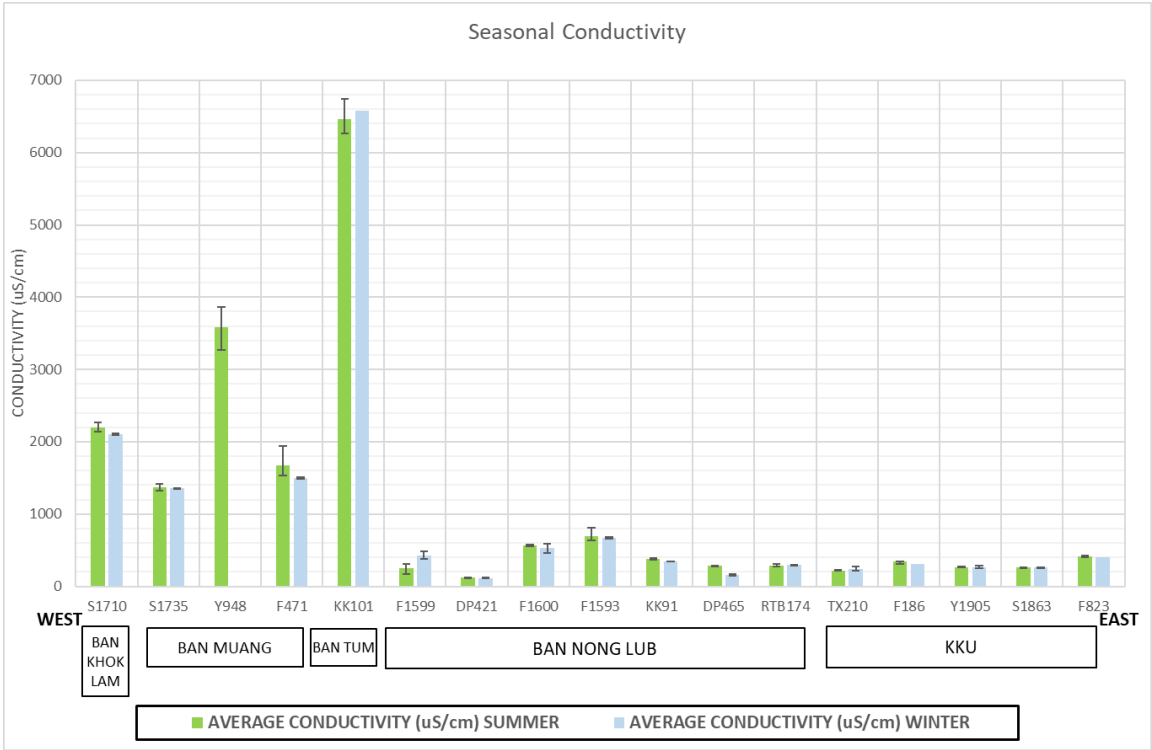
Figure 4.6 Seasonal variations in fluid conductivity.

4.4 ERT Profiles

Ban Muang Site

The Ban Muang ERT profile is oriented northwest to southeast south of well Y948 in the western region of the study area (Figure 4.7). The profile's length is 235 meters. This transect is closest to well Y948.
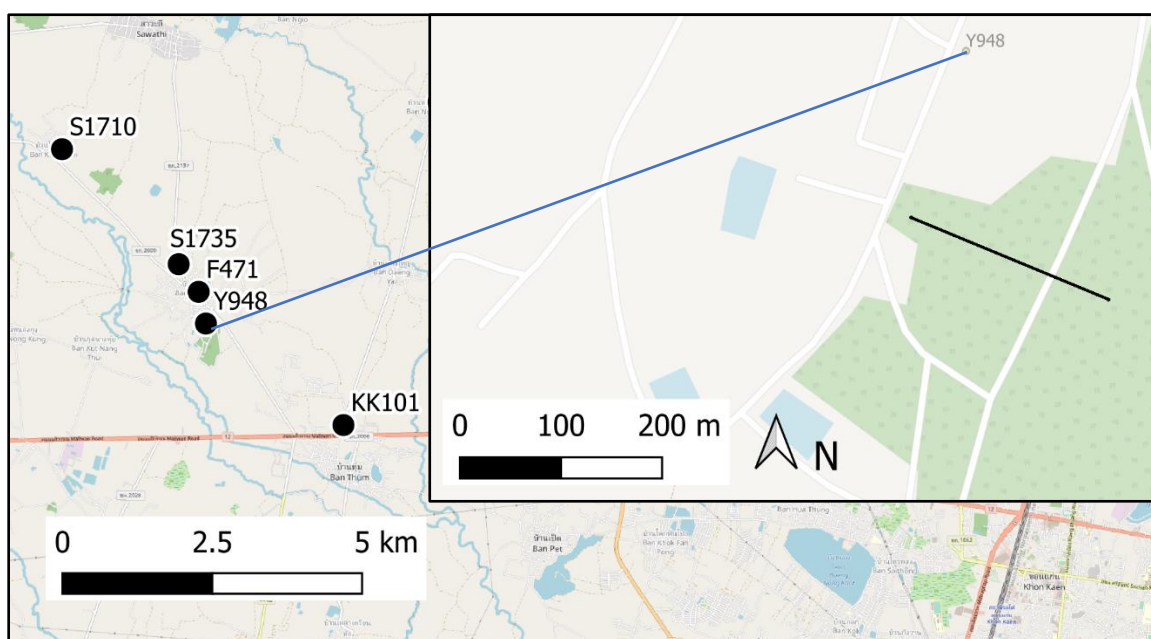
Figure 4.7 Location of Ban Muang ERT line. The ERT line is in black in the inset and the blue line connects the location of well Y948 on the map with its location on the inset.

The resistivity scale is approximately 0 to 500 ohm-meters on the Ban Muang site profile. The depth of the profile is 40 meters (Figure 4.8). While the majority of the profile is characterized by low resistivity, the resistivity is highest close to the ground surface. This high resistivity layer is in the upper 2.5-to-5 meters for most of the profile and is 7.5

meters above the rainy season water table.

The geology of the Ban Muang site is characterized by an upper yellow-brown, clayey sand, a middle layer of light-yellow silty clay and sand, then a lower layer of reddish-brown sand based on lithologic logs from nearby wells (Figure 4.8). The top of the water table during the rainy season is between the clay layer and lower sand layer and is within the lower sand layer during the dry season. A conductive blocky blue to dark blue region appears in the 5-to-20-meter depth region of the profile and lies between the dry season water table and the bottom of the upper sand layer. Measurements from wells Y948, F471, and S1735 were used for the conductivity values, and water level measurements from wells F471, S1735, and S1710 were used for this diagram. The groundwater in wells located near the Ban Muang site, closest to the transect, is more saline than water from the eastern portion of the study area. The wells in this area include Y948, F471, and S1735 and are among the most conductive of the sampled wells.
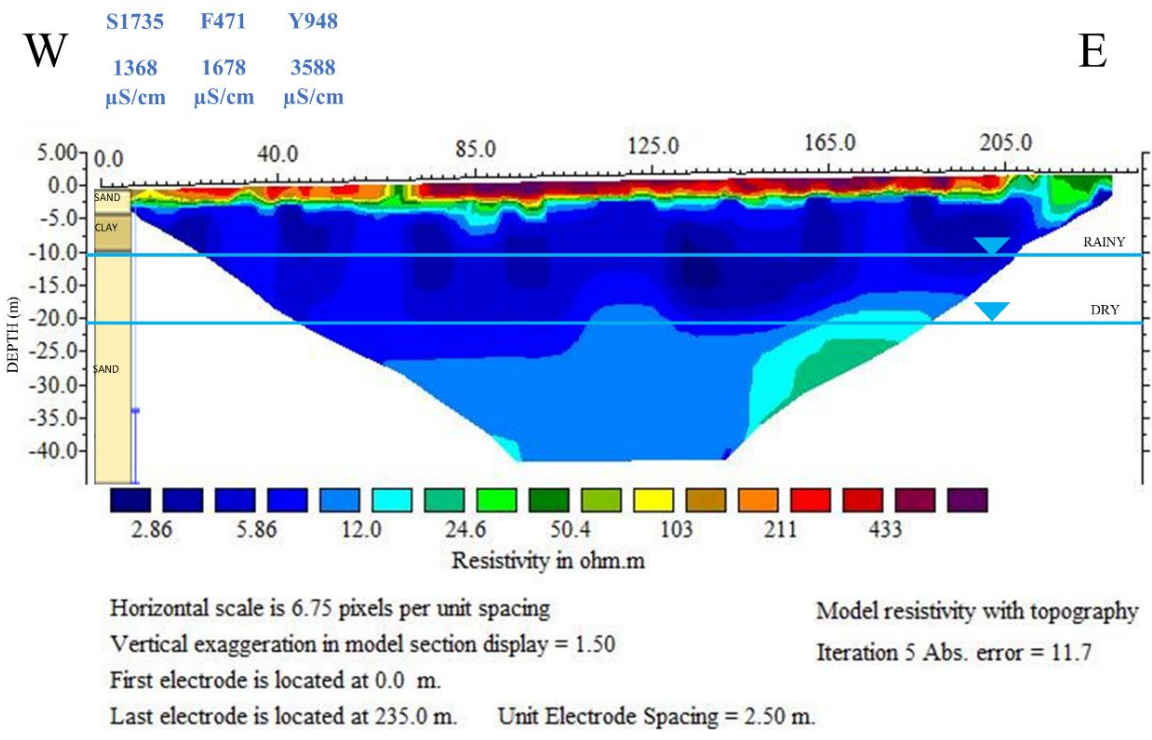
Figure 4.8 Ban Muang site. Horizontal and vertical distances are in meters. ERT profile,

lithology, seasonal water level measurements, and fluid conductivity at labeled well

locations in blue at top of profile.

Bannonglub Site

The Bannonglub ERT profile is oriented from northwest to southeast (Figure 4.9). The profile is 415 meters long and is located very close to wells F1600, F1593, and KK91. The profile is also near wells DP421 and DP465, which were sampled for groundwater conductivity and water levels.
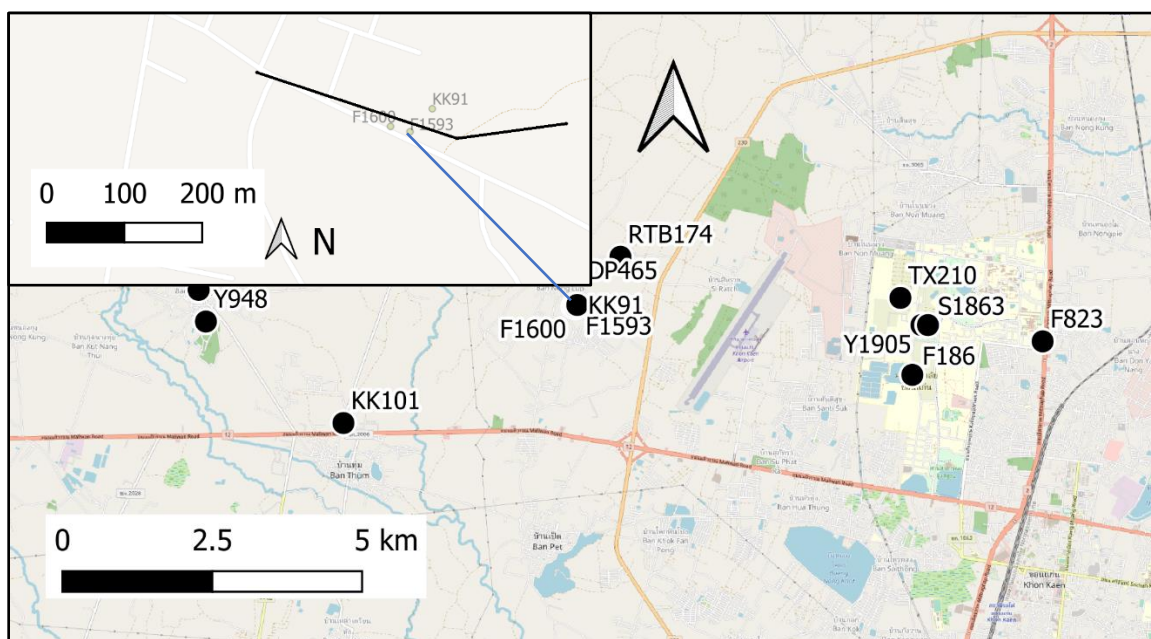
Figure 4.9 Location of Bannonglub ERT line, which runs between wells F1600, F1593, and KK91. The ERT line is in black, in the inset. The blue line connects the location of well F1593 on the map with its location on the inset.

The Bannonglub profile is 60 meters deep. Resistivity is high (conductivity is low) along the ground surface, particularly in the eastern part of the profile. This high resistivity

layer is the upper 2.5-to-5 meters and is 4 to 5 meters above the rainy season water table. A large, round high resistivity (low conductivity) zone is noted approximately 280 m from the west side of the profile. This feature is near a dry creek bed and a parallel road runs perpendicular to the profile line. This highly resistive area may represent an air-filled void, such as a culvert, under the road.

On this diagram, wells F1600 and F1593 are superimposed on the ERT profile (Figure 4.10). According to the lithologic logs, well F1600 consists of a top layer of topsoil, underlain by clay. The characteristics of the middle clay layer are unknown, and the lower clay layer is described simply as "brown clay". Well F1593 is reported to be an upper clay layer underlain by red, sandy shale. During the rainy season, the water table is at the interface between the topsoil and upper clay layer in well F1600 and between the clay and shale in well F1593. The dry season water table is through the middle clay in well F1600 and shale in well F1593. Conductivity measurements in wells F1600, F1593, and KK91, and water level measurements in wells F1600, KK91, DP421 were used in this comparison.
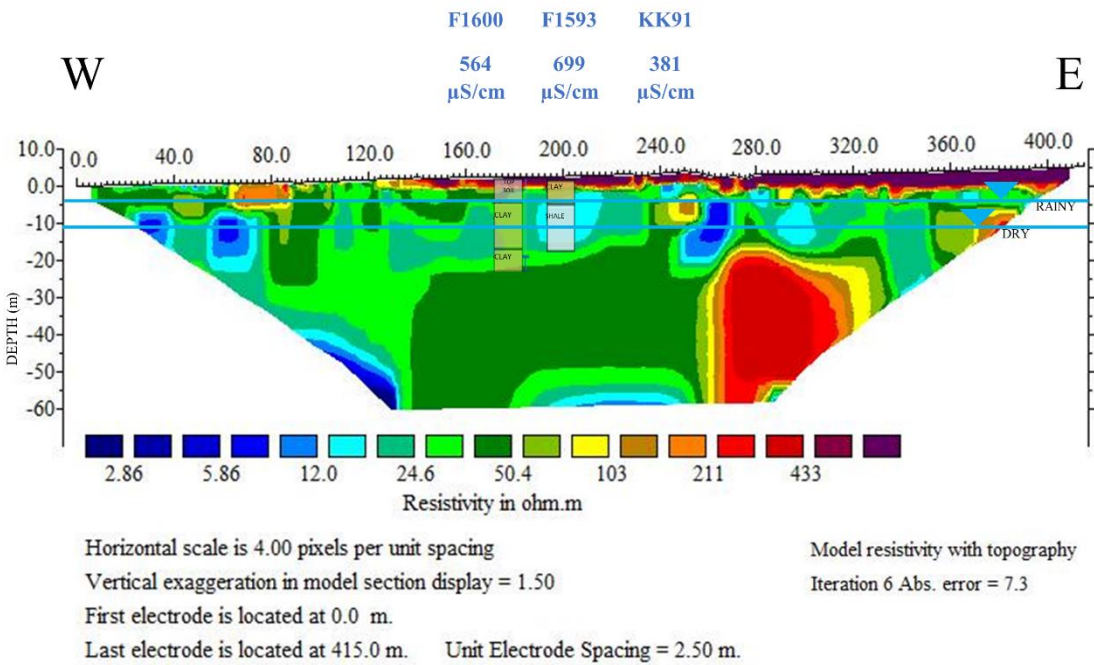
Figure 4.10 Bannonglub site. Horizontal and vertical distances are in meters. ERT

profile, lithology, seasonal water level measurements, and fluid conductivity at labeled

well locations in blue at top of profile.

CHAPTER 5

DISCUSSION

5.1 Resistivity and Conductivity Interpretations

According to the resistivity scales on the ERT profiles, dark blue to blue represents materials with low resistivity and highly resistive materials are red to dark purple. Higher resistivity values appear to coincide with lower groundwater conductivity measurements in nearby wells and vice-versa. Brackish-saline and fresh groundwater was measured in close proximity to predominantly low-resistivity and high resistivity ERT profiles, respectively. A steep resistivity gradient is observed at 2.5 m depth at the fresh groundwater site, and at 5 m depth at the saline groundwater site, which do not coincide with the water table depth. On both ERT profiles there is higher resistivity in the uppermost layer and lower resistivity below. Since saturated sediments are more conductive than unsaturated, the lower layer may be saturated.

The Ban Muang site diagram may reflect the difference between the upper sand and the underlying clay layer with lower resistivity because clay usually has a lower resistivity than sand. The conductive region between the middle clay layer and lower sand layer in the Ban Muang ERT profile may represent lateral variations in lithology. Alternately, this region could signify an older water table level that may have left behind conductive minerals or represent a seasonal capillary fringe, where NaCl has precipitated in the unsaturated zone.

The subsurface conditions appear to be more homogeneous at the Ban Muang site than at the Bannonglub site. The majority of the Ban Muang profile depicts resistivity from 6 to 12 ohm-meters. Since an increase in clay content, salinity, and water generally reflect low resistivity, a saline alluvial aquifer is expected to have low resistivity, akin to the results for Ban Muang. Likewise, the converse is evident for the fresher Bannonglub profile.

The groundwater of Bannonglub School, in the eastern portion of the study area, is fresher than in the western portion of the study area. The ERT profile of this area displays variable resistivity horizontally and vertically. The water from nearby wells F1600, F1593, KK91, DP421, and DP465 are less conductive than the wells of the other site. The estimated water table depth at this location is 5 meters. The difference in geology of wells F1600 and F1593 may be reflected on this profile. On the ERT profile, the shale is within a slightly lower resistivity than the location of the clay. Although the resistivity of shale is within the resistivity values for clay, the resistivity variations may reflect lithological variations.

Subsurface materials of both ERT profiles are most likely composed of clay, silt, and sand alluvial sediments. Laterite has a reported average resistivity of 1200 ohm-meters (Tajudin et. al., 2017). The description of the pisolitic and gravelly laterite in the study area is closest in character to the massively bedded rock and coarse dry sand and gravel deposits values, which are normally in the high 1000s, and still within the acceptable range for laterite resistivity (Burger, et. al., 2006, Tajudin et. al., 2017). Although laterite is present

in the study area, since the resistivity values are all under 1,000 ohm-meters, it is not likely

present along the ERT profiles. Sandstone does exist here, but at deeper depths. For both

profiles, the lithology is mainly fine-grained, and there is probably not conglomerate, dry

gravel, massively bedded or fractured rock, although the presence of shale is possible

(Table 4).

Table 4 Applicable Resistivity Values (Burger, et. al., 2006, Tajudin et. al., 2017).

Material	Resistivity ($\Omega{\cdot}m$)
Clay	5- 100
Sand/ clay	6- 350
Sand	50- 500
Laterite	960- 19,000
Shale	7- 40
Sandstone	70- 900
Conglomerate	900- 10,000
Wet to moist clayey soil and wet clay	1s to 10s
Wet to moist silty soil and silty clay	Low 10s
Wet to moist silty and sandy soils	10s to 100s
Sand and gravel with layers of silt	Low 1000s
Coarse dry sand and gravel deposits	High 1000s
Well-fractured to slightly fractured rock with moist, soil-filled cracks	100s
Slightly fractured rock with dry, soil-filled cracks	Low 1000s
Massively bedded rock	High 1000s

Since conductivity is the inverse of resistivity, the equation, $c = \frac{1}{\rho}$, in SI units of

S/m and ohm-meters is used to convert fluid conductivity (*c*) measurements into resistivity

(ρ) units. The first three columns are resistivity in units of μS/cm, parts per million, and

S/m (Table 5). The unit used for resistivity is the ohm-meter. Fresh water has a resistivity

of 9 to 100 ohm-meters, brackish, between 1 and 9 ohm-meters, and saline, 0.3 to 1 ohm-

meter (Sikandar and Christen, 2012). According to these classifications, twelve of

seventeen wells are considered fresh water and the remaining five are brackish.

Table 5 Conductivity and Resistivity of Tested Wells

WELL NAME	AVERAGE CONDUCTIVITY (μS/cm)	AVERAGE CONDUCTIVITY (ppm)	AVERAGE CONDUCTIVITY (S/m)	AVERAGE RESISTIVITY (ohm-m)
S1710	2197	1099	0.220	5
S1735	1368	684	0.137	7
F471	1678	839	0.168	6
Y948	3588	1794	0.359	3
KK101	6458	3229	0.646	2
F1599	251	126	0.025	40
DP421	118	59	0.012	85
F1600	564	282	0.056	18
F1593	699	350	0.070	14
KK91	381	191	0.038	26
DP465	282	141	0.028	35
RTB174	288	144	0.029	35
TX210	220	110	0.022	45
F186	339	170	0.034	29
Y1905	268	134	0.027	37
S1863	267	134	0.027	37
F823	417	209	0.042	24

The alluvial deposits of ancient rivers cut into floodplain terrace deposits and left

sand, silt, and clay. The finer-grained deposition of Quaternary alluvium of the western

wells are more saline than those of coarser terrace deposits. The western wells are part of

a structural syncline, and the eastern wells are part of a structural anticline. The presence of a syncline may indicate that the western wells would be farther above the Mahasarakham Formation than the eastern wells (Arjwech et al, 2018; Srisuk, 1996). However, the Khorat Group, including the Mahasarakham Formation, is uplifted to the west of the study area and to some degree, saline water from higher elevations in the west is transported to low-lying areas in the (south)east.

The Impact of Capillary Rise on Resistivity

Fine-grained soil textures at both locations are likely to promote capillary rise and the upward migration of saline pore water in unsaturated sediments. Based on values for different soils, several meters of capillary rise (Table 6) are possible in the study area. The bottom of the high resistivity ERT zones are 2-5 m and 8 m above the rainy season water tables at fresh and saline groundwater sites, respectively. These measurements are consistent with observations of capillary rise heights of other authors. Since ERT values are a function of clay content, water content, and fluid salinity, differences in values in the unsaturated sediments at both locations may reflect variations of soil moisture or clay content. The resistivity differences may be caused by unsaturated sediments overlying saturated sediment or possibly a layer of topsoil with higher resistivity. The irregular boundary may represent a capillary fringe associated with heterogeneous sediments. At the Bannonglub site, the irregular boundary may represent the capillary fringe. At the Ban Muang site, this irregular pattern may represent a capillary fringe, although 8 m may be higher than the several meters normally attributed to capillary rise in clay. Here, the

irregular pattern could be areas where the upward movement of saline water resulted in

precipitation of minerals or possibly a representation of varied sediment textures. The

repeated cyclic seasonal upward movement of saline water and precipitation of salts may

also be responsible for the irregular resistivity boundary. The results indicate that

seasonal and long-term water level trends should be considered when evaluating

resistivity measurements in saline subsurface conditions, which are essential to successful

salinity management.

Table 6 Estimated capillary rise heights in study area wells.

WELL NAME	WATER TABLE DEPTH	LITHOLOGY AT AND ABOVE WATER TABLE	ESTIMATED CAPILLARY RISE
S1710	6.7	Clay and sand	50 cm (0.5 m) up to several meters
S1735	10.8	Shale	80 cm (0.8 m) up to several meters
Y948	9.9	Clay	80 cm (0.8 m) up to several meters
F1599	2.2	Topsoil	100 cm (1 m)-300 cm (3 m)
F1600	5.2	Topsoil	100 cm (1 m)-300 cm (3 m)
F186	2.8	Clay	80 cm (0.8 m) up to several meters
Y1905	6.8	Laterite, with clay above	1.5 cm (0.015 m)
S1863	9.2	Laterite, with clay above	1.5 cm (0.015 m)
F823	2.0	Sand	50- 80 cm (0.5- 0.8 m)

5.2 Regional Differences in Water Table Levels and Groundwater Conductivity

Water Level Elevations During Dry and Rainy Seasons

Water levels were measured during the rainy and dry seasons and the results were used to create water table elevation contour maps (Figures 5.1 and 5.2). The contoured water table surface maps display elevation contour lines at regular intervals, 5 meters in this case. During the rainy season, the water table is deeper in the southeastern part of the study area than elsewhere (Figure 5.1). The apparent groundwater flow based on this limited dataset is from the northwest to the south and southeast.

Average seasonal water level measurements determined that the water table dropped by approximately 11 m at Ban Muang and 5 m at Ban Muang between the rainy season to the dry season. During the dry season there is little to no rainfall in the study area and the dry season water elevation map has a different appearance than the rainy season map (Figure 5.2). The groundwater still generally flows to the south, but round areas of lower elevation appear in the middle of the map, to the west and east of the study area. These are regions of topographic lows which may be more pronounced given the dry conditions.
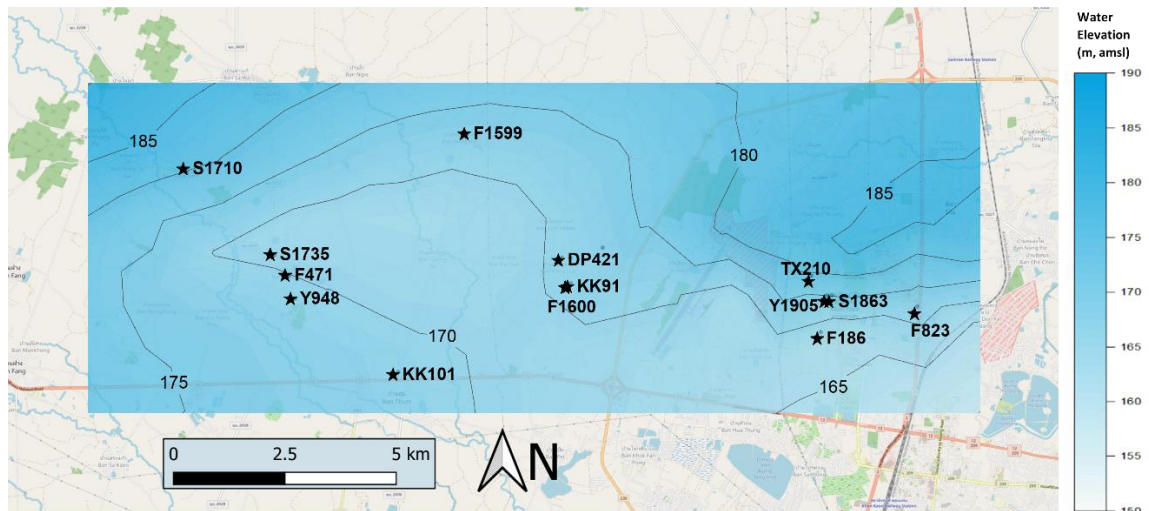
Figure 5.1 Rainy Season Groundwater Levels and wells sampled. White and light blue areas depict a shallower water table, and as blue becomes darker, the water table is deeper (OriginPro, 2020; QGIS, 2019).
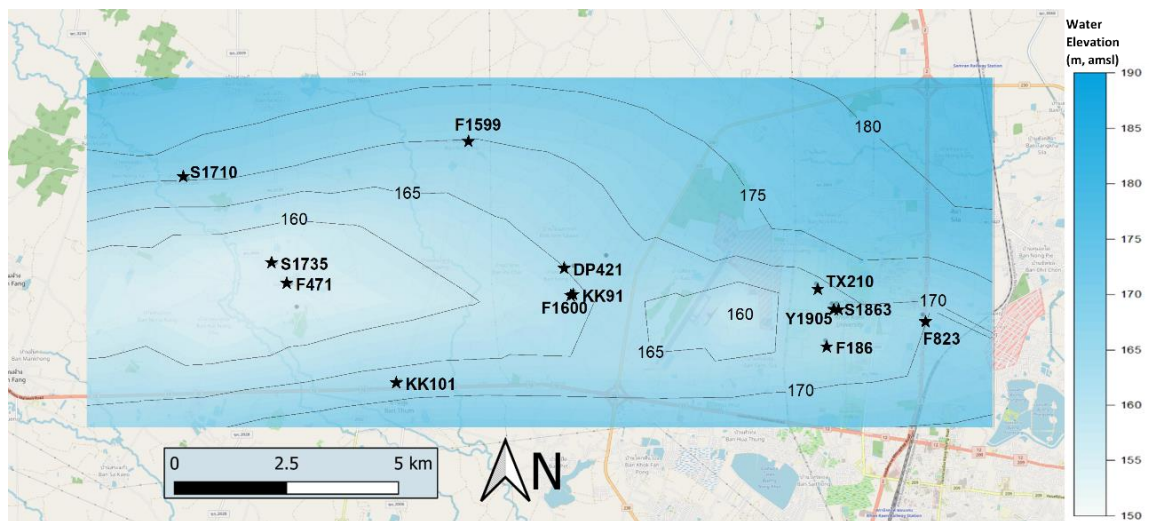
Figure 5.2 Dry Season Groundwater Levels and wells sampled.. White and light blue areas depict a shallower water table, and as blue becomes darker, the water table is deeper (OriginPro, 2020; QGIS, 2019).

Ground Conductivity Maps

Conductivity measurements from the rainy and dry seasons were used to create salinity contour maps (Figures 5.3 and 5.4). Given the relationship between salinity and conductivity, the salinity contour maps illustrate that the fluid conductivity, and therefore groundwater salinity is higher in the southwest and lower in the northeast part of the study area. Overall, the seasonal maps are very similar. The wells to the west are situated in Quaternary alluvium deposits and appear to have more saline water than those to the east. The wells to east are Quaternary terrace deposits and the water here is fresher.

Sixteen wells were used to obtain water samples during the rainy and dry seasons. Twelve wells had higher conductivity in the rainy season and four wells had more conductive water samples in the dry season. Elevated conductivity during the rainy season supports the idea that salt accumulates in the unsaturated zone as a result of capillary rise and then dissolves as the water table rises.
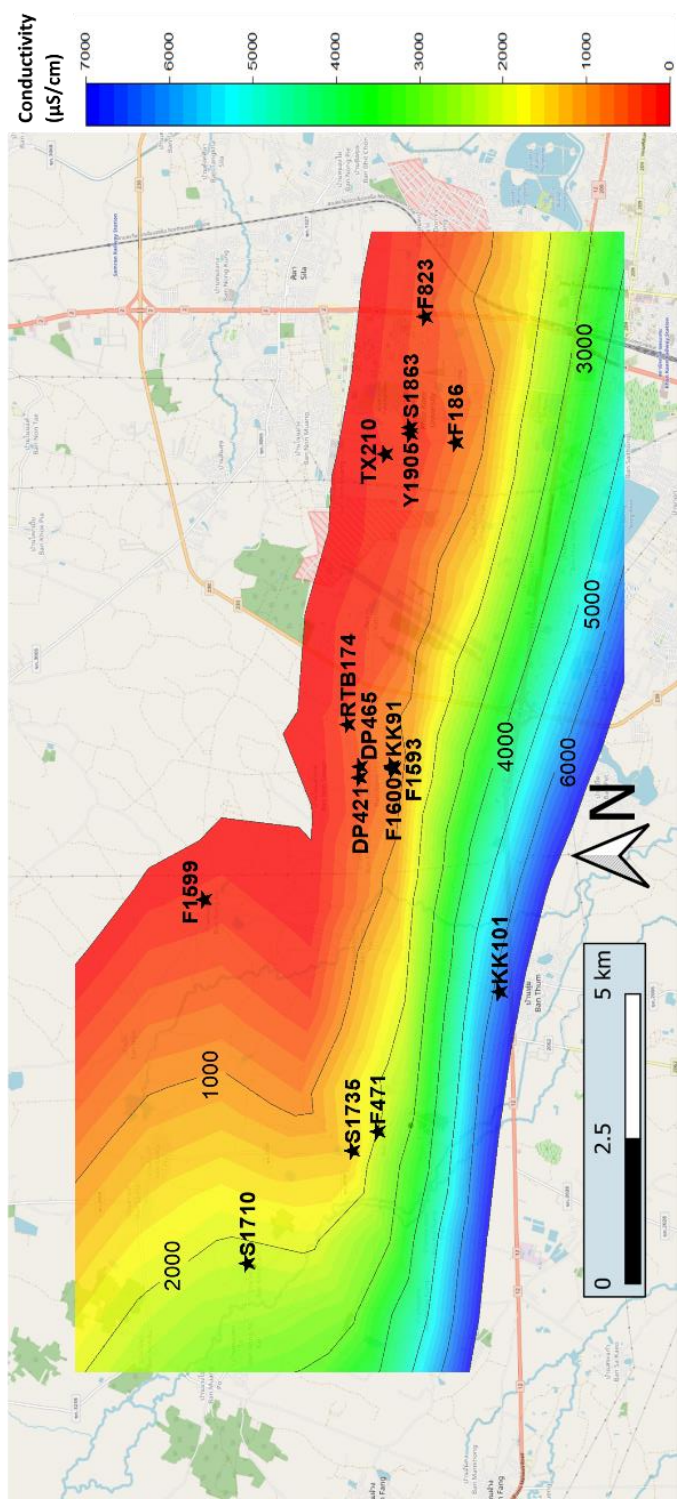
Figure 5.3 Rainy Season Groundwater Salinity and wells sampled. Blues indicate high conductivity/salinity, and red indicates low conductivity/salinity (OriginPro, 2020; QGIS, 2019).
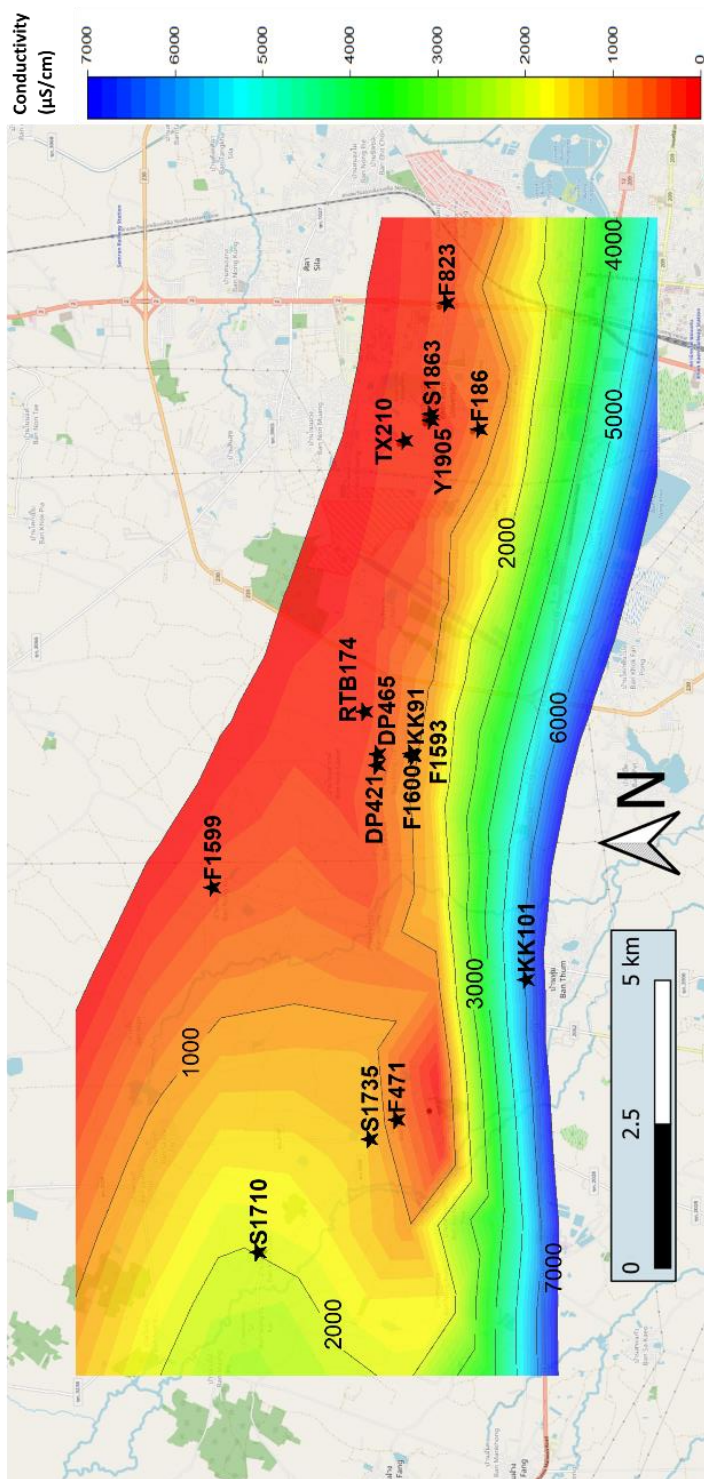
Figure 5.4 Dry Season Salinity Contour Map. Wells and contour intervals are labelled. Blues indicate high conductivity/salinity, and red indicates low conductivity/salinity (OriginPro, 2020; QGIS, 2019).

CHAPTER 6

CONCLUSIONS

6.1 Summary

Fresh water is universally necessary for drinking and for agricultural use. Since salt-affected soil affects people in over 100 countries, understanding its origin and learning mitigation techniques is essential to providing for the increasing water needs of increasing populations, especially as the problem is exacerbated by human activity and climate change. Therefore, a multidisciplinary approach, specifically combining geophysical and hydrological methods, assists in the evaluation, understanding, and management of salt-affected regions.

Water conductivity and levels were measured during rainy and dry seasons. Water levels were recorded in 13 wells seasonally. All wells had higher levels in the rainy season, with an average of an 8 m drop between the rainy and dry seasons. Water levels dropped 5 m and 10 m at the Bannonglub site and Ban Muang site, respectively. Seasonal conductivity measurements were taken from water sampled from 16 wells. In 12 wells, conductivity was higher in the rainy season than in the dry season. Four wells contained water that had higher conductivity in the dry season. The rainy season average conductivities ranged from 118 to 6458 µS/cm and between 117 and 6580 µS/cm in the dry season. The difference between the average rainy and dry season conductivity measurements is between 1 and 179 µS/cm. Specific conductance differed between the rainy and dry seasons by 34 µS/cm and 97 µS/cm at the Bannonglub site and Ban Muang

site, respectively.

The study area has a western more saline groundwater zone and an eastern fresher groundwater zone. Both the ERT surveys and specific conductivity values reflect the distinction between salinity conditions. A likely capillary fringe is apparent on the ERT profiles, given the resistivity values and water table levels. ERT can be useful in identifying the top of the water table and the top of the capillary zone, especially in combination with direct measurements taken at water wells. The results affirm that resistivity of ERT profiles agree with conductivity measurements of water from nearby wells. Brackish-saline and fresh groundwater was found in close proximity to predominantly low resistivity and high resistivity ERT profiles, respectively.

The water table is not responsible for steep ERT resistivity gradients at depths of 8 m at the western (saline) site and 2.5-5 m at the eastern (fresh) site. The water table at the eastern site during the rainy season corresponds to horizontal resistivity variations, but the western profile does not. Fine-grained soil textures at both locations promote capillary rise in unsaturated sediments. Modelled capillary rise estimates are consistent with the positions of the ERT resistivity gradients at both locations. For these reasons, ERT can be useful to identify the top of the water table in fresh-water aquifers and the top of the capillary zone in saline aquifers.

6.2 Future Work

The results indicate that seasonal and long-term water-level trends should be considered when evaluating resistivity measurements in saline subsurface conditions. ERT profiling may be useful for identifying the top of the water table or capillary zone where both saline and freshwater conditions exist but should be supported by water table and fluid salinity measurements. Based on this study, seasonal and long-term water-level and groundwater salinity trends should be considered when evaluating ERT data.

Since the local geology is complex, confidence in the lithology would provide more confidence in the interpretation of resistivity data. Future research would benefit from the collection of well borings along the ERT profiles and where water is tested.to better determine the relationship between lithology and resistivity. Upcoming research would benefit from a greater number of ERT lines and situating them as close as possible to water sampling wells. Seasonal studies including ERT and groundwater measurements throughout the year could assist in understanding cycles of salinization and specifically the role of capillary rise in this process. This understanding is key to salinity management.

Civil engineering projects in salt-affected regions would benefit from the inclusion of salinity studies to lessen negative effects of salinity on infrastructure. Although a building may be above the water table, its foundation may lie within the capillary zone and still be subjected to corrosive conditions. Since saline water and soil damage building materials, understanding the height of capillary rise may be beneficial to civil engineering projects in salt-affected areas with high water tables.

These findings are relevant to the management of dryland salinity regions that are impacted by long-term climatic change and variations in seasonal rain patterns. The estimated time needed to enact a management plan is between 30 and 50 years (Hall et al., 2004). Agricultural efforts to adapt to salinization, such as the introduction of salt tolerant crops, addition of natural fertilizers, and the reintroduction of native halophytes and trees would benefit from an understanding of the depth of saline soil (Arunin and Pongwichian, 2015). Irrigation leads to elevating the water table, therefore, lowering the water table would reduce soil salinization (Loffler and Kubiniok, 1988). Introducing crops that need less water may decrease the need for irrigation, thus lowering the water table. Fluctuations in water table elevations caused by changing irrigation patterns may promote unsaturated zone salinization. The use of ERT methods for understanding the distribution and origin of saline soil and identifying mitigation techniques may help resolve the increasing water needs of increasing populations, especially as the problem is exacerbated by human activity and climate change.

Hall et al. (2004) recommend an interdisciplinary and international approach to the issue, which would include professionals from earth sciences, economists, agriculture, and social sciences. Given that other countries, such as Australia, experience dryland salinity and much research has been done there, that knowledge could be applied in Thailand (Hall et al., 2004). In the past, a lack of data has been a limitation of management, and cooperation could mitigate that problem (Hall et al., 2004).

REFERENCES

Arjwech, R., Everett, M., and Wanakao, P., 2018, The relationship between geological factors and the distribution of saline soil; a case study in Khon Kaen Basin, Thailand, in EGU General Assembly Conference Abstracts, April 2017, v. 19, p. 5861.

Arjwech, R., Everett, M., and Schulmeister, M., 2020, Soil salinity mapping of an urbanizing area in northeastern Thailand: Quarterly Journal of Engineering Geology and Hydrogeology, v. 53, p. 413–424, doi.org/10.1144/qjegh2019-113.

Arjwech, R., Everett, M., and Wanakao, P., 2019, The relationship between geological factors and the distribution of saline soil: A case study in the Khon Kaen Basin of Thailand: Songklanakarin Journal of Science & Technology, v. 41, no. 5, p. 974-983.

Arunin, S. and Pongwichian, P., 2015, Salt-affected soils and management in Thailand. Bulletin of the Society of Sea Water Science: Special Issue: Salt Damage and Food Production of the World, v. 69, p. 319-325.

Bluecover Location Based Technology, 2019, GPS Waypoints Mobile Application: https://www.bluecover.pt/.

Boonsener, M., 1985, Review on Quaternary geology of Khon Kaen Province, Northeastern, Thailand. Conference on geology and mineral resources development of the Northeast, Thailand, p. 229-233.

Briški, M. Stroj, A., Kosovi, I., and Borovi, S., 2020, Characterization of aquifers in metamorphic rocks by combined use of electrical resistivity tomography and monitoring of spring hydrodynamics: Geosciences, v. 10, n. 137, doi:10.3390/geosciences1004013.

Brouwer, C., Goffeau, A., and Heibloem, M., 1985, Food and Agriculture Organization of the United Nations (FAO) Land and Water Development Division Irrigation Water Management: Training Manual No. 1: Introduction to Irrigation: http://www.fao.org/3/r4082e/r4082e00.htm (accessed April 2019).

Buaphan., C., Youngme., W., Wannakao, L., Buapeng, S., Tassanasorn, A., and Sriboonlue, Y., 1995, Groundwater origin investigation with isotopic compositions for evaluations of high productive deep aquifers in Khon Kaen area, Thailand: Hydrogeology in Proceedings of the International Conference on Geology, Geotechnology and Mineral Resources of Indochina (Geo-Indo 1995), November 22-25, 1995: Khon Kaen, Thailand.

Burger, H., Sheehan, A., and Jones, C., 2006. Introduction to Applied Geophysics:

Exploring the Shallow Subsurface: New York, W.W. Norton, 554 p.

Cement Concrete & Aggregates Australia, 2018, Industry Guide T56: Residential Slabs and Footings in Saline Environments: https://www.ccaa.com.au/documents/INDUSTRY_GUIDE_T56_Residential_Slabs_and_Footings_in_Saline_Environments.pdf (accessed November 2021).

Dauphin, L. and Patel, K., 2020, NASA Earth Observatory image using soil moisture data from NASA-USDA and the SMAP Science Team: https://earthobservatory.nasa.gov/images/146293/drought-hits-thailand (accessed March 2021).

Electricity Generating Authority of Thailand, 2013, Information: Ubol Ratana Dam: https://www.egat.co.th/en/index.php?option=com_content&view=article&id=56&Itemid=117 (accessed June 2021).

El Tabakh, M., Utha-Aroon, C., Schreiber, B. C., 1999, Sedimentology of the Cretaceous Maha Sarakham evaporites in the Khorat Plateau of northeastern Thailand: Sedimentary Geology v. 123, p. 31–62. doi:10.1016/S0037-0738(98)00083-9.

Fetter, C.W., 1994, Applied Hydrogeology, 3rd Edition: New York, Macmillan College Publishing Company, 691 p.

Fetter, C. W., 2001, Applied Hydrogeology, 4th ed.: Upper Saddle River, N.J.: Prentice Hall, 598 p.

Foley, J., Greve, A., Huth, N., Silburn, M., 2012, Comparison of soil conductivity measured by ERT and EM38 geophysical methods along irrigated paddock transects on Black Vertosol soils in Proceedings of the 16th ASA Conference: Capturing Opportunities and Overcoming Obstacles in Australian Agronomy, October 14-18, 2012: Armidale, Australia: www.agronomy.org.au (accessed November 2021).

Food and Agriculture Organization of the United Nations and Intergovernmental Technical Panel on Soils (FAO and ITPS), 2015, The Status of the World's Soil Resources Main Report: Rome, Italy: http://www.fao.org/3/i5199e/i5199e.pdf (accessed April 2019).

Food and Agriculture Organization of the United Nations (FAO), 2016, AQUASTAT website: http://www.fao.org/nr/water/aquastat/countries_regions/THA/ (accessed April 2019).

Galazoulas, E.C., Mertzanides, Y.C., Petalas, C.P., and Kargiotis, E.K., 2015, Large scale electrical resistivity tomography survey correlated to hydrogeological data for mapping groundwater salinization: a case study from a multilayered coastal aquifer in Rhodope, Northeastern Greece: Environmental Processes, v. 2, p. 19–

35, doi:10.1007/s40710-015-0061-y.

Greggio, N., Giambastiani, B., Balugani, E., Amaini, C., and Antonellini, M., 2018, High-resolution electrical resistivity tomography (ert) to characterize the spatial extension of freshwater lenses in a salinized coastal aquifer: Water, v. 10, doi:10.3390/w10081067.

Hall, N., Lertsirivorakul, R., Greiner, R., Yongvanit, S., Yuvaniyama, A., Last, R., and Milne-Home, W., 2004, Land use and hydrological management: ICHAM, an integrated model at a regional scale in northeastern Thailand: International Congress on Environmental Modelling and Software 2nd International Congress on Environmental Modelling and Software: Osnabrück, Germany.

Hanna Instruction Manual HI 98121: https://hannainst.com/downloads/dl/file/id/1742/manHI_98121.pdf (accessed November 2019).

Haworth, H., Javanaphet, J., Jumchet, C., and Chiangmai, P., 1959, Report on ground water exploration and development of the Khorat Plateau region: Prepared in cooperation with the United States Operations Mission to Thailand, Thailand Royal Department of Mines, Ground Water Bulletin No. 1: Bangkok, Thailand, 72 p.

Inkscape Project version 0.92.5, 2020, open-source software: https://inkscape.org/ (accessed June 2020).

Jansen, J., 2011, Geophysical Methods to Map Brackish and Saline Water in Aquifers, in Proceedings of the 2011 Georgia Water Resources Conference, April 11-13, 2011: Athens, Georgia.

Lamoreaux, P., Charaljavanaphet, J., Jalichan, N., Chiengmai, P., Bunnag, D., Thavisri, A., and Rakprathum, C., 1958, Reconnaissance of the geology and ground water of the Khorat Plateau, Thailand: U.S. Geological Survey Water-Supply Paper 1429.

Löffler, E., & Kubiniok, J., 1988, Soil salinization in north-east Thailand (Bodenversalzung in Nordost-Thailand): Erdkunde, v. 42, no. 2, p. 89-100.

Marks, D., 2019, Water access and resilience to climate-induced droughts in the Thai secondary city of Khon Kaen: Unequal and unjust vulnerability, in Daniere, A. et al., eds., Urban Climate Resilience in Southeast Asia: Switzerland, Springer International Publishing, p. 41-62.

Miller, R., Wesley L. Bradford, W., and Peters, N., 1988, Specific Conductance: Theoretical Considerations and Application to Analytical Quality Control: U.S. Geological Survey Water-Supply Paper 2311,

https://pubs.usgs.gov/wsp/2311/report.pdf (accessed November 2021).

Najib, S., Fadili, A., Mehdi, K., Riss, J., and Makan, A., 2017, Contribution of hydrochemical and geoelectrical approaches to investigate salinization process and seawater intrusion in the coastal aquifers of Chaouia, Morocco: Journal of Contaminant Hydrology, v. 198, p. 24-36, doi:10.1016/j.jconhyd.2017.01.003.

Oakton Instruction Manual Multi-Parameter Testr 35, 2010: http://www.4oakton.com/SellSheets/35425-00,-05,-10.pdf (accessed November 2019).

Office of the National Economic and Social Development Council, 2017, Khon Kaen City Municipality Project for Promoting Sustainability in Future City of Thailand: http://www.nesdb.go.th/download/document/Brochure%20of%20Khon%20Kaen%20Town%20Municipality.pdf (accessed October 2019).

OriginPro, Version 2020 (Learning Edition), OriginLab Corporation, Northampton, MA, USA.

Patcharapreecha, P., Topark-Ngarm, B., Goto, I., and Kimura, M., 1990, Studies on saline soils in Khon Kaen region, Northeast Thailand: I. Physical and chemical properties of saline: Soil Science and Plant Nutrition, v. 35, no. 2, p. 171-179.

QGIS Development Team, 2019, QGIS Geographic Information System. Open Source Geospatial Foundation Project: http://qgis.osgeo.org.

Raksaskulwong, R. and Monjai, D., 2007, Relationship between the Mahasarakham Formation and high terrace gravels along the Khon Kaen-Kalasin provinces in GEOTHAI'07 International Conference on Geology of Thailand: Towards Sustainable Development and Sufficiency Economy.

Riwayat, A., Nazri, M., and Abidin, M., 2018, Application of electrical resistivity method (ERM) in groundwater exploration in IOP Conference Series: Journal of Physics: Conference Series 995, doi :10.1088/1742-6596/995/1/012094.

Rusydi, A. F., 2017, Correlation between conductivity and total dissolved solid in various type of water: A review in IOP Conference Series: Earth and Environmental Science, Global Colloquium on GeoSciences and Engineering. October 2017: Bandung, Indonesia. v. 118.

Seeboonruang, U., 2013, Relationship between groundwater properties and soil salinity at the Lower Nam Kam River Basin in Thailand: Environmental Earth Science: Springer-Verlag Berlin Heidelberg, v. 69, p. 1803–1812, doi:10.1007/s12665-012-2012-5.

Shen, L., Siritongkham, N., Wang, L., Liu, C., Nontaso, A., Khadsri, W., and Hu, Y,

2021. The brine depth of the Khorat Basin in Thailand as indicated by high-resolution Br profile. Sci Rep. 2021 Apr 21;11(1):8673. doi: 10.1038/s41598-021-88037-6. PMID: 33883638; PMCID: PMC8060250.

Sikandar, P. and Christen, E.W., 2012, Geoelectrical sounding for the estimation of hydraulic conductivity of alluvial aquifers: Water Resources Management, v. 26, n. 5, p. 1201-1215, doi:10.1007/s11269-011-9954-3.

Srisuk, K., 1996, Surface water and ground-water salinity in the Khon Kaen drainage basin, Northeast Thailand: International Symposium on Geology and Environment, p. 243- 254.

Syscal R1 Plus multi-electrode imaging system: http://www.iris-instruments.com/Pdf_file/Resistivity_Sounding/summary_of_operation.pdf (accessed February 2020).

Tajudin, S. A. A., Suied, A. a., Ezree, A. M., Nizam, Z. M., Madun, A., Hazreek, Z. A. M., sunar, N. M., and Embong, Z., 2017, The use of electrical resistivity method to mapping the migration of heavy metals by electrokinetic: IOP Conference Series: Materials Science and Engineering, v. 226, no. 1, doi:10.1088/1757-899X/226/1/012062.

Thailand Department of Groundwater Resources, 2019: http://www.dgr.go.th/th/home.

Thailand Meteorological Department, 2015, The Climate of Thailand: https://www.tmd.go.th/en/archive/thailand_climate.pdf (accessed April 2019).

Thailand Meteorological Department, 2019- 2020, Meteorological Information Section Upper Northeast Meteorological Center Monthly district rain schedule: http://www.khonkaen.tmd.go.th/rainmet_kk.php?fbclid=IwAR2LaXxGXnedn3SE J21UtzyDHs7Pxnxmo3Ow1MYtvTuz3SgdxKLV1W2G7d4 (accessed November 2019- January 2020).

timeanddate.com. Annual weather averages in Khon Kaen, Thailand based on weather reports collected during 2005– 2015: https://www.timeanddate.com/weather/thailand/khon-kaen/historic (accessed September 2019).

United States Environmental Protection Agency (EPA), 2003, Office of Water, Health and Ecological Criteria Division., Drinking Water Advisory: Consumer Acceptability Advice and Health Effects Analysis on Sodium: https://www.epa.gov/sites/production/files/2014-09/documents/support_cc1_sodium_dwreport.pdf (accessed May 2021).

United States Geological Survey (USGS), 2021, Water Science School: Saline Water and Salinity: https://www.usgs.gov/special-topic/water-science-school/science/saline-water-and-salinity?qt-science_center_objects=0#qt-science_center_objects

(accessed May 2021).

Wada, H., 2005, Chemical properties and their effect on productivity in Proceedings, Session 3 of Management of Tropical Sandy Soils for Sustainable Agriculture: A holistic approach for sustainable development of problem soils in the tropics. November 27- December 2, 2005: Khon Kaen, Thailand: http://www.fao.org/3/AG125E11.htm (accessed April 2019).

Williams, L.J. and Spechler, R.M., 2011, Aquifer mapping project in the southeastern United States in Proceedings of the Georgia Water Resources Conference: University of Georgia April 11–13, 2011.

Williamson, D., Peck, A., Turner, J., and Arunin, S., 1989, Groundwater hydrology and salinity in a valley in northeast Thailand: Groundwater Contamination in Proceedings of the Symposium held during the Third IAHS Scientific Assembly: Baltimore, MD, May 1989, IAHS Publ. no. 185, p. 147-154.

Wongsawat, S., Dhanesvanich, O., and Panjasutaros, S., 1992, Groundwater resources of northeastern Thailand in Proceedings of the National Conference on Geologic Resources of Thailand: Potential for Future Development, November 17-24, 1992: Bangkok, Thailand.

Wongsomsak, S., 1986, Salinization in northeast Thailand: Japanese Journal of Southeast Asian Studies, v. 24, no. 2, p. 133-153, doi:10.20495/tak.24.2.

Yamaguchi, K., 2020, Iron isotope compositions of Fe-oxide as a measure of water-rock interaction: An example from Precambrian tropical laterite in Botswana: Frontier Research on Earth Evolution, v. 2 (accessed October 2020).

APPENDIX A

Lithologic Logs

The lithologic logs were made available from the Thailand Department of Groundwater Resources (2019) and include well name, depths, rock types, lithologic descriptions, locations, and in some cases, well depths and screened intervals. These logs were used to construct geologic cross sections and Google Earth elevations were used to assist in this process.

CROSS SECTION A TO A'										
WELL NAME	GOOGLE EARTH ELEVATION (ON PROFILE)	FROM DEPTH (m)	TO DEPTH (m)	ROCK 1	ROCK 2	LITHOLOGIC DESCRIPTION	EASTING	NORTHING	DRILL DEPTH (m)	SCREENED INTERVAL (m)
Y1919	176	0	5	top soil		top soil	269670	1821860	64	60
		5	17	sand	clay	fine sand clay				
		17	23	gravel	sand	gravel sand				
		23	26	clay		brown clay				
		26	57	shale		shale				
		57	64	clay		brown clay				
F823	171	0	6	sand		Sand, brown, fine to coarse grained	268496	1821597	6	15-21
		6	8	gravel		Gravel, yellowish brown				
		8	20	clay		Clay, yellowish brown, sandy				
		20	21	clay		Clay, reddish brown, silty				
F185	192 (180)	0	6	clay		clay	267691	1822292	25	69-78
		6	9	clay		clay				
		9	29	clay		clay				
		29	32	gravel		gravel+ pebble				
		32	52	clay		clay				
		52	72	clay		clay				
		72	76	gravel		gravel + pebble				
		76	82	shale		shale				
S1863	190 (188)	0	2	top soil		top soil	266454	1822114	54	40-49, 50-53
		2	7	sand		fine sand				
		7	8	clay		sandy clay				
		8	34	laterite		laterite				
		34	54	clay		clay				
Y1905	188	0	2	top soil		top soil	266473	1821910	50	37-46
		2	6	sand	clay	sandy clay				
		6	21	laterite		laterite				
		21	38	clay		brown clay				
		38	47	gravel	sand	gravel sand				
		47	50	clay		brown clay				
S1707	189 (180)	0	2	top soil		top soil	265266	1822100	60	16-20, 36-39, 39-43
		2	24	clay	sand	clay + sand				
		24	33	sand		sand				
		33	60	shale		shale				
F1282	206 (188)	0	14	shale		red shale	264370	1822961	16	
		14	23	gravel	sand	gravel + sand				
		23	55	clay		red clay				
F1593	181 (169)	0	6	clay		clay	260698	1822215	24	
		6	18	shale		red sandy shale				

CROSS SECTION A TO A' (continued)											
F1600	181 (169)	0	5	top soil		top soil	260673	1822222	24	20-24
		5	18	clay		clay				
		18	24	clay		brown clay				
F457	162	20	26	clay		yellow sandy clay	258200	1822440	23	
		26	27	clay	shale	red shale + yellow sandy clay				
		27	35	clay		yellow sandy clay				
		35	44	clay		sandy lay and gray sandy clay				
		44	67	sandstone		sandstone				
		67	76	shale	sandstone	brown shale + sandstone				
F1598	183	0	5	top soil		top soil	254692	1822370	30	24-30
		5	15	clay		clay + pebble				
		15	24	clay		yellow clay				
Y948	183	0	5	sand		yellowish brown, clayey	254529	1821968	15	36-48
		5	11	clay		light yellow, silty				
		11	49	sand		reddish brown, calcareous				
L942	183	0	3	clay		clay = reddish brown, gravelly	251581	1821849	7	18-24
		3	24	siltstone		siltstone = reddish brown, brittle				
F1592	185	0	6	top soil		top soil	251492	1821825	39	36-39
		6	18	shale		brown shale				
		18	39	shale		brown shale				
S1735	185	0	2	top soil		top soil	254075	1822957	48	28-32, 36-40, 44-48
		2	3	clay		clay				
		3	8	clay	sand	clay + sand				
		8	48	shale		shale				
F186	169	0	6	clay		clay	266320	1821078	25	58.5-76.5
		6	9	clay		clay				
		9	29	clay		clay				
		29	32	gravel		gravel + pebble				
		32	38	gravel		pebble				
		38	54	clay		clay				
		54	66	clay		clay				
		66	72	clay		clay				
		72	76	gravel		gravel + pebble				
		76	82	shale		shale				

CROSS SECTION B TO B'									
WELL NAME	GOOGLE EARTH ELEVATION (ON PROFILE)	FROM DEPTH (m)	TO DEPTH (m)	ROCK 1	ROCK 2	LITHOLOGIC DESCRIPTION	EASTING	NORTHING	DRILL DEPTH (m)	SCREENED INTERVAL (m)
U836	178	0	2	top soil		top soil	254350	1826400	6	15-21
		2	3	laterite		laterite				
		3	18	sand	clay	yellow sandy clay				
		18	21	clay		brown clay				
Y1932	193	0	5	top soil		top soil	251919	1827322	50	
		5	24	clay		clay				
		24	30	clay		brown clay				
		30	48	clay		yellow clay				
		48	50	sand	clay	sandy clay				
F1596	185	0	5	clay		clay	252686	1826934	30	24-30
		5	12	clay		clay				
		12	18	clay		yellow clay				
		18	24	clay		clay				
		24	30	shale		shale				
F1177	186	0	2	top soil		top soil	253506	1826810	15	42-48
		2	9	clay		white clay				
		9	12	clay		clay				
		12	27	sand		sand				
		27	49	clay		clay				
F1594	190	0	2	top soil		top soil	251174	1826689	30	24-30
		2	9	clay		clay				
		9	15	clay		yellow clay				
		15	27	clay		yellow clay				
		27	36	clay		white clay				
		36	75	clay		brown clay				
F1589	185	0	9	clay		yellow clay	253251	1826703	36	30-36
		9	24	clay						
		24	33	sand						
		33	36	clay						
S743	183	0	2	top soil		top soil	251496	1825013	5	
		2	5	clay	sand	sand + clay				
		5	8	clay		yellow clay				
		8	14	clay	sand	clay + sand				
		14	15	shale		shale				
S1709	186	0	2	top soil		top soil	251927	1824881	52	32-36, 40-44, 48-52
		2	6	clay	sand	clay + sand				
		6	30	shale		shale				
		30	52	shale		hard shale				
S1710	187	0	2	top soil		top soil	252139	1824873	72	42-48, 66-72
		2	8	clay	sand	clay + sand				
		8	45	shale		shale				
		45	52	shale	clay	shale + clay				
S1704	187	0	2	top soil		top soil	252159	1824838	33	16-20, 24-28
		2	6	sand	gravel	sand + gravel				
		6	21	gravel	clay	gravel + clay				
		21	30	sandstone		sandstone				
		30	60	sandstone		sandstone				

CROSS SECTION B TO B' (continued)										
S1735	188	0	2	top soil		top soil	254075	1822957	48	28-32, 36-
		2	3	clay		clay				40, 44-48
		3	8	clay	sand	clay + sand				
		8	48	shale		shale				
F1598	183	0	5	top soil		top soil	254692	1822370	30	24-30
		5	15	clay						
		15	24	clay						
Y948	183	0	5	sand		yellowish brown, clayey	254529	1821968	15	36-48
		5	11	clay		light yellow, silty				
		11	49	sand		reddish brown, calcareous				
L942	183	0	3	clay		clay = reddish brown, gravelly	251581	1821849	7	18-24
		3	24	siltstone		siltstone = reddish brown, brittle				
F1592	185	0	6	top soil		top soil	251492	1821825	39	36-39
		6	18	shale		brown shale				
		18	39	shale		brown shale				
F1154	169	0	2	clay		clay	256575	1819852	11	30-36
		2	11	shale		brown shale				
		11	24	shale		hard brown shale				
		24	37	shale		hard brown shael				
F1152	179	0	2	top soil		top soil	251492	1821825	39	36-39
		2	3	clay		yellow clay				
		3	12	shale		red shale				
		12	15	shale		hard red shale				
		15	30	shale		hard red shale				
		30	43	shale		hard red shale				
F1153	180	0	2	top soil		top soil	253296	1818551	15	42-48
		2	3	clay		clay				
		3	5	clay		yellow clay				
		5	30	shale		red shale				
		30	49	shale		red shale				
F176	169	0	2	clay		clay	256897	1816643	20	
		2	66	shale		shale				

CROSS SECTION C TO C'										
WELL NAME	GOOGLE EARTH ELEVATION (ON PROFILE)	FROM DEPTH (m)	TO DEPTH (m)	ROCK 1	ROCK 2	LITHOLOGIC DESCRIPTION	EASTING	NORTHING	DRILL DEPTH (m)	SCREENED INTERVAL (m)
L940	178	0	5	sand		sand = yellowish, fine sand	258418	1825657	7	20-24
		5	18	clay		clay = yellowish and r=yellowish brown; sandy				
F1599	181	0	1	top soil		top soil				
		1	5	clay		clay	258418	1825657	7	20-24
		5	7	clay		yellow clay				
L794	175	0	11	top soil	clay	top soil + sandy clay	258331	1825331	9	24-30
		11	21	clay		clay				
		21	30	sandstone		sandstone				
F457	162	20	26	clay		yellow sandy clay	258200	1822440	23	
		26	27	clay	shale	red shale + yellow sandy clay				
		27	35	clay		yellow sandy clay				
		35	44	clay		sandy clay and gray sandy clay				
		44	67	sandstone		sandstone				
		67	76	shale	sandstone	brown shale + sandstone				
F1600	181 (169)	0	5	top soil		top soil	260673	1822222	24	20-24
		5	18	clay		clay				
		18	24	clay		brown clay				
F1593	181 (169)	0	6	clay		clay	260698	1822215	24	
		6	18	shale		red sandy shale				
PW8650	157	0	3	silt		Silt, brown	260301	1818002	90	
		3	8	silt	clay	Silt & Clay, light brown				
		8	13	sand		Sand, brown, very fine to medium -grained				
		13	24	clay	sand	Clay & Sand				
		24	38	sand		Sand, gray				
		38	43	clay		Clay, gray				
		43	51	sand		Sand, gray				
		51	84	clay		Clay, gray				
F232	155	0	6	clay		clay	260500	1817840	5	10.5-16.5
		6	9	gravel		gravel				
		9	12	gravel		pebble				
		12	18	clay		clay				
F1284	167	0	3	clay		yellow clay	263622	1816638	11	30-36
		3	37	shale		red shale				
F857	167	0	2	gravel	clay	yellowish brown, limonite stained	263796	1816437	7	18-24
		2	5	clay		yellowish red, limonite stained				
		5	8	clay		yellowish red, limonite stained				
		8	24	shale		reddish brown, calcareous				

APPENDIX B

Data Tables and pH Chart

Appendix B includes the field data chart listing well names, locations, and descriptions made available from the Thailand Department of Groundwater Resources (2019). This information includes field and lab measurements such as water table elevations, pH and conductivity water sample measurements, temperatures, elevations, along with field notes concerning port samples and pumping information. Also included are the seasonal conductivity table and seasonal pH table and chart.

Field Data

KHON KAEN, THAILAND FIELD AND LAB MEASUREMENTS AND LOCATIONS

STUDY AREA	WELL NAME	DATE	LITHOLOGIC LOGS AVAILABLE	EASTING	NORTHING	WATER LEVEL (m)	SCREENED INTERVAL (m)	STICK UP LEVEL (m)	WELL DEPTH (m)	OAKTON pH	OAKTON: pH TEMPERATURE (degrees celcius)	OAKTON: CONDUCTIVITY (microsiemens/cm)	OAKTON: CONDUCTIVITY TEMPERATURE (degrees celcius)	HANNA: CONDUCTIVITY (microsiemens/cm)	HANNA TEMPERATURE (degrees celcius)	ELEVATION AT GROUND (PHONE APP)	FIELD NOTES
	F1600	5/19/2019	Y	260673	1822222	5.3	20-24	0.58	24	7.47	21.9	555	19.5	489	20 (LAB)	176.2	PUMP OFF
		5/24/2019				5.12				7.35	29.3	564	29.3	541	29.8		PUMP OFF
		5/27/2019				5.28				7.02	29.1	572	29.2	552	29.1		PUMP OFF
		5/31/2019				5.11				7.69	30.9	555	31.3	508	32.9		
		11/25/2019				5.13				6.82	28.9	588	28.8				
		2/4/2020				7.5				6.5	28.6	463	29				
		3/19/2020				23											PUMPING
	F1593	5/24/2019	Y	260698	1822215	22.96		0.26	24	6.68	28.7	641	28.7	621	28.7	178.2	PUMPING
		5/27/2019				23.79				6.7	28.7	809	28.7	760	28.9		PUMPING
		5/31/2019				21.48				6.62	29.1	646	29.1	604	31		PUMPING
		11/25/2019				17.17				6.5	28.4	687	28.2				PUMP OFF
		2/4/2020				5.4				6.54	28	658	27.9				PUMP OFF
		3/19/2020				17.5											PUMPING
	KK91	5/24/2019	N	260727	1822244	4.68		0.6	29	6.49	28.4	391	28.3	378	28.8	177.2	PUMP OFF
		5/27/2019				5.04				6.54	28.5	384	28.6	369	28.8		PUMP OFF
		5/31/2019				4.39				6.6	28.6	368	28.8	352	30		
		11/25/2019				5.03				6.8	27.9	342	27.7				
		2/4/2020				4.56				6.74	27.8	342	27.8				
		3/19/2020				5.22											
	DP421	5/19/2019	N	260526	1822831	2.62	24-30	0.28	32	6.48	21.6	117	17.7	102	17.7 (LAB)	172.2	PUMP OFF
		5/24/2019				2.5				6.3	28.8	123	28.7	120	29.3		PUMP OFF
		5/27/2019				2.45				6.36	28.7	115	28.7	111	28.5		PUMP OFF
		11/25/2019				2.51				7.01	28.7	118	28.7				
		2/4/2020				3.9				7.02	28.6	115	28.9				
		3/19/2020				3.23											
Ban Nong Lub	DP465	5/19/2019	N	260719	1822820	35.56	45-51	0.36	53	6.35	21.2	284	18.9	261	18.9 (LAB)	177.2	PUMPING, PORT
		5/24/2019				4.05				6.21	29.6	281	29.4	269	30.1		PUMP OFF, WL HIGH, PORT
		5/27/2019				34.83				6.63	29.7	281	29.6	267	30.1		PUMPING, PORT
		11/25/2019				38.38				6.15	28.9	173	28.8				PUMPING
		2/4/2020				35.07				6.03	29.2	142	29				PUMPING
		3/19/2020				27.81											PUMPING
	RTB174	5/21/2019	N	261448	1823047	30.3	74-80	0.48	84	6.56	30.5	308	30.6	285	30.6	213.2	PORT
		5/24/2019				22.79				6.67	28.9	280	28.9	265	30	206	PUMP OFF
		5/27/2019				27.16				6.67	29.8	276	29.8	264	30.3		PUMPING, PORT
		11/25/2019				22.84				6.16	30.3	286	30.2				PUMP OFF
		2/4/2020				28.28				6.75	28.9	299	29				PUMPING
	5704D008	5/21/2019	N	262703	1823137	20 (database)	51-54	0.4	58	7.02	31	970	30.9	880	31.9	212.16	PORT
		5/24/2019								7.25	27.3	918	27.3	872	27.4		PORT
		11/25/2019															
	F1599	5/28/2019	Y	258418	1825657	2.43	20-24	0.4	24	6.81	29.7	313	29.1	299	28.6	174.3	PUMP OFF
		5/31/2019				2.12				6.28	30.4	170	30.6	158	32.9		
		6/1/2019				2.14				6.68	29.6	269	29.6	253	30.8		
		11/26/2019				2.3				6.78	28.5	478	28.5				
		2/4/2020				2.67				6.72	27.7	373	27.9				
		3/19/2020				2.8											

KHON KAEN, THAILAND FIELD AND LAB MEASUREMENTS AND LOCATIONS

STUDY AREA	WELL NAME	DATE	LITHOLOGIC LOGS AVAILABLE	EASTING	NORTHING	WATER LEVEL (m)	SCREENED INTERVAL (m)	STICK UP LEVEL (m)	WELL DEPTH (m)	OAKTON pH	OAKTON: pH TEMPERATURE (degrees celcius)	OAKTON: CONDUCTIVITY (microsiemens/cm)	OAKTON: CONDUCTIVITY TEMPERATURE (degrees celcius)	HANNA: CONDUCTIVITY (microsiemens/cm)	HANNA TEMPERATURE (degrees celcius)	ELEVATION AT GROUND (PHONE APP)	FIELD NOTES
	Y1905	5/19/2019	Y	266473	1821910	6.3	37-46	0.94	50	5.88	21.4	270	19.4	244	19.4 (LAB)	173.1	PUMP OFF
		6/1/2019				7.8				6.07	29.8	274	29.9	265	29.8		PUMP OFF
		6/7/2019				6.15				5.99	28.8	260	28.9	257	28.7		PUMP OFF
		9/9/2019				7.98				5.91	29.3	283	29.1				PUMP OFF
		11/25/2019				8.37				5.98	29.3	251	29				PUMP OFF
		3/19/2020				7.45											
	F186	5/19/2019	Y	266320	1821080	2.8	58.5-76.5	0.6	81	6.35	23	348	20.2	424	20.2 (LAB)		PUMP OFF
		6/1/2019				3.09				6.41	29.2	336	29.2	310	31.1		PUMP OFF
		6/7/2019				2.41				6.37	28.1	333	28.2	310	27.9		PUMP OFF
		9/9/2019				1.61				6.47	29.1	308	29.2				PUMP OFF
		11/25/2019				2.91				6.41	29.7	310	29.7				
KKU	F823	5/19/2019	Y	268496	1821638	2.24	15-21	0.15	21	6.46	22.8	406	20.9	311	20.9 (LAB)		PUMP OFF
		6/6/2019				2.12				6.45	28.9	413	29	389	29.1		
		6/7/2019				1.71				6.65	29.2	431	29.4	404	28.6		
		11/25/2019								6.55	29.7	404	29.6				
	S1863	6/1/2019	Y	265581	1821909	9.16	40-49, 50-53	0.41	54	6.27	29.7	266	29.7	262	31.4		PUMP OFF
		6/6/2019				9.15				6.08	29.3	268	29.3	258	30.7		PUMP OFF
		6/7/2019				9.13				6.2	29	266	28.9	260	27.6		PUMP OFF
		9/9/2019				8.73				6.18	29.4	264	29.4				PUMP OFF
		11/25/2019				9.13				6.12	29.6	258	29.7				PUMP OFF
		3/19/2020				10.21											
	TX210	6/1/2019	N	266122	1822362	11.32	48-54	0.44	58	6.17	30.6	222	30.8	208	32.7		PUMP OFF
		6/6/2019				11.36				5.8	29.4	219	29.5	211	31.9		
		6/7/2019				11.32				6.08	28.6	218	28.6	212	29.3		
		9/9/2019				11.28				6.19	28.9	272	29				PUMP OFF
		11/25/2019				11.3				6.11	29.6	211	29.6				
Ban Kok	TX93	5/21/2019	N	265582	1816074	15.4	34-42	0.37	42	7.23	32.8	913	32.9	839	33.9	160.08	PUMPING, PORT
		5/31/2019				6.66				7.4	31	888	30.7	816	32.9		PUMP OFF

KHON KAEN, THAILAND FIELD AND LAB MEASUREMENTS AND LOCATIONS

STUDY AREA	WELL NAME	DATE	LITHOLOGIC LOGS AVAILABLE	EASTING	NORTHING	WATER LEVEL (m)	SCREENED INTERVAL (m)	STICK UP LEVEL (m)	WELL DEPTH (m)	OAKTON pH	OAKTON: pH TEMPERATURE (degrees celcius)	OAKTON: CONDUCTIVITY (microsiemens/cm)	OAKTON: CONDUCTIVITY TEMPERATURE (degrees celcius)	HANNA: CONDUCTIVITY (microsiemens/cm)	HANNA TEMPERATURE (degrees celcius)	ELEVATION AT GROUND (PHONE APP)	FIELD NOTES
Ban Tum	KKI01	5/28/2019	N	256825	1820277	7.7		0.4	26	6.89	29.7	6270	29.7	TOO HIGH	28.5	177.3	PUMP OFF
		5/31/2019				5.07				6.77	30.6	6540	30.7	TOO HIGH	33.9		PUMP OFF
		6/1/2019				4.48				6.78	29.7	6280	29.6	TOO HIGH	29.9		PUMP OFF
		6/6/2019				16.88				6.73	29.3	6740	29.5	TOO HIGH	29.2		PUMPING
		11/26/2019				4.72				6.8	29.2	6580	29.3				PUMP OFF
		3/19/2020				1.1											
	F457	5/28/2019	Y	258200	1822440	-	-	-	-	7.45	31.2	1235	31.4	1187	30.7	164.2	PORT, POND
		5/31/2019				-				7.16	32.9	1246	33.1	1178	33		
		6/1/2019								7.24	32.9	1234	33	1179	33		
	Y948	5/28/2019	Y	254529	1821968	9.95	36-48	0.31	49	6.52	29.4	3860	29.5	3637	29	181	PUMP OFF
		5/31/2019				9.91				6.76	29.1	3580	29.1	3345	30.3		
		6/1/2019				9.9				6.7	29	3270	29	3561	28.3		
		6/6/2019				9.87				6.37	28.7	3640	28.7	3600	28.7		
		11/26/2019				-				-	-	-	-				WELL CLOSED
Ban Muang	F471	5/28/2019	N	254408	1822496	9.44	28.5-34.5	0.36	46.5	8.75	30.2	1537	30.1	1458	29.3	179.3	PUMP OFF
		5/31/2019				9.37				8.48	31	1551	31.3	1400	30.3		
		6/1/2019				9.4				7.76	30.1	1945	30.1	1905	31.8		
		11/26/2019				10.37				8.71	30	1509	29.9				
		2/4/2020				10.85				8.36	29.7	1488	29.6				
		3/19/2020				11.3											
	S1735	5/28/2019	Y	254075	1822957	10.8	28-32	0.66	48	7.7	29.7	1415	29.7	1331	31.3	178.3	PUMP OFF
		5/31/2019				10.78				8.21	29.9	1364	30.3	1286	30.3		
		6/1/2019				10.82				8.2	29.5	1325	29.5	1286	30.3		
		11/26/2019				12.05				7.13	29.3	1352	29.6				
		2/4/2020				12.5				7.35	29.3	1353	29.3				
		3/19/2020				13											
Ban Khok Lam	S1710	5/31/2019	Y	252127	1824872	6.68	12-18, 42-48, 66, 72	0.24	72	7.15	29.7	2270	29.6	2059	30.7		PUMP OFF
		6/1/2019				6.56				7.34	28.9	2180	29	2050	30.1		
		6/6/2019				6.73				7.04	28.3	2140	28.3	2040	28.2		
		11/26/2019				7.28				7.08	28.6	2090	28.4				
		2/4/2020				9.46				6.99	28	2120	28.2				
		3/19/2020				11.23											

Seasonal Conductivity Data Table

	Seasonal Conductivity Data									
WELL NAME	AVERAGE CONDUCTIVITY (uS/cm) SUMMER	AVERAGE CONDUCTIVITY (uS/cm) WINTER	SUMMER HIGH	SUMMER LOW	WINTER HIGH	WINTER LOW	SUMMER POSITIVE ERROR	SUMMER NEGATIVE ERROR	WINTER POSITIVE ERROR	WINTER NEGATIVE ERROR
S1710	2197	2105	2270	2140	2120	2090	73	57	15	15
S1735	1368	1353	1415	1325	1353	1352	47	43	1	1
Y948	3588		3860	3270			273	318		
F471	1678	1499	1945	1537	1509	1488	267	141	11	11
KK101	6458	6580	6740	6270			283	188		
F1599	251	426	313	170	478	373	62	80	53	53
DP421	118	117	123	115	118	115	5	3	1	1
F1600	564	526	572	555	588	463	8	9	63	63
F1593	699	673	809	641	687	658	110	58	15	15
KK91	381	342	391	368	342	342	10	13	0	0
DP465	282	158	284	281	173	142	2	1	16	16
RTB174	288	293	308	276	299	286	20	12	7	7
TX210	220	242	222	218	272	211	2	2	31	31
F186	339	309	348	308			9	31		
Y1905	268	267	274	260	283	251	6	8	16	16
S1863	267	261	268	266	264	258	1	1	3	3
F823	417	404	431	406			14	11		

Seasonal pH Data Table

Seasonal pH Data										
WELL NAME	SUMMER pH AVERAGE	WINTER pH AVERAGE	SUMMER HIGH	SUMMER LOW	WINTER HIGH	WINTER LOW	SUMMER NEGATIVE ERROR	SUMMER POSITIVE ERROR	WINTER NEGATIVE ERROR	WINTER POSITIVE ERROR
S1710	7.18	7.04	7.34	7.04	7.08	6.99	0.14	0.16	0.04	0.04
S1735	8.04	7.24	8.21	7.70	7.35	7.13	0.34	0.17	0.11	0.11
Y948	6.59		6.76	6.37			0.22	0.17		
F471	8.33	8.54	8.75	7.76	8.71	8.36	0.57	0.42	0.18	0.18
KK101	6.79	6.80	6.89	6.73			0.06	0.10		
F1599	6.59	6.75	6.81	6.28	6.78	6.72	0.31	0.22	0.03	0.03
DP421	6.38	7.02	6.48	6.30	7.02	7.01	0.08	0.10	0.00	0.00
F1600	7.38	6.66	7.69	7.02	6.82	6.50	0.36	0.31	0.16	0.16
F1593	6.67	6.52	6.70	6.62	6.54	6.50	0.05	0.03	0.02	0.02
KK91	6.54	6.77	6.60	6.49	6.80	6.74	0.05	0.06	0.03	0.03
DP465	6.40	6.09	6.63	6.21	6.15	6.03	0.19	0.23	0.06	0.06
RTB174	6.63	6.46	6.67	6.56	6.75	6.16	0.07	0.04	0.30	0.30
TX210	6.02	6.15	6.08	5.80	6.19	6.11	0.22	0.06	0.04	0.04
F186	6.38	6.44	6.41	6.35	6.47	6.41	0.03	0.03	0.03	0.03
Y1905	5.98	5.95	6.07	5.88	5.98	5.91	0.10	0.09	0.04	0.04
S1863	6.18	6.15	6.27	6.08	6.18	6.12	0.10	0.09	0.03	0.03
F823	6.52	6.55	6.65	6.45			0.07	0.13		
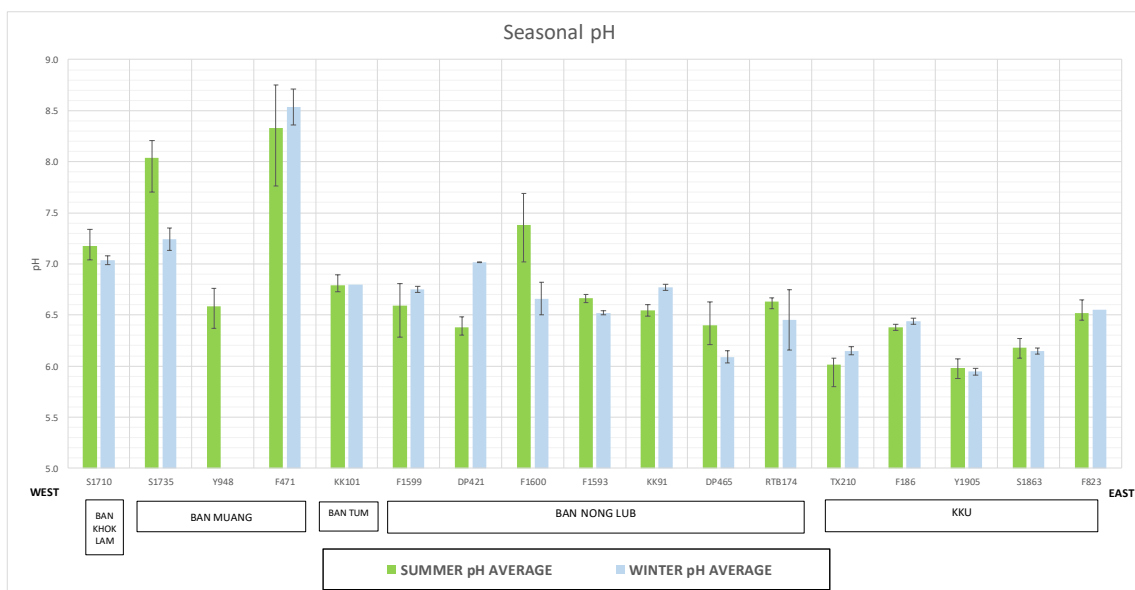
I, <u>Brooke Molson-Moran</u>, hereby submit this thesis to Emporia State University as partial fulfillment of the requirements for an advanced degree. I agree that the Library of the University may make it available to use in accordance with its regulations governing materials of this type. I further agree that quoting, photocopying, digitizing or other reproduction of this document is allowed for private study, scholarship (including teaching) and research purposes of a nonprofit nature. No copying which involves potential financial gain will be allowed without written permission of the author. I also agree to permit the Graduate School at Emporia State University to digitize and place this thesis in the ESU institutional repository, and ProQuest Dissertations and Thesis database and in ProQuest's Dissertation Abstracts International.

<u>Brooke Molson-Moran</u>
Signature of Author

<u>12/9/2021</u>
Date

<u>Investigating Seasonal Impacts on Subsurface Salinization in Northeastern Thailand with Electrical Conductivity Tomography</u>
Title of Thesis